



ONTARIO GEOLOGICAL SURVEY

Geophysical Data Set 1076

Ontario Airborne Geophysical Surveys
Magnetic and Electromagnetic Data
Nestor Falls Area

by

Ontario Geological Survey

2014

Ontario Geological Survey
Ministry of Northern Development and Mines
Willet Green Miller Centre, 933 Ramsey Lake Road,
Sudbury, Ontario P3E 6B5 Canada

Contents

Disclaimer.....	v
Citation.....	v
1. Introduction.....	1
2. Survey Location And Specifications.....	1
2.1. Survey Location.....	1
2.2. Topographic Relief and Cultural Features.....	3
2.3. Survey And System Specifications.....	3
2.4. Data Acquisition.....	4
2.4.1. Flight Line Specifications.....	4
2.4.2. Survey Operations.....	4
3. Survey Area Geology.....	5
4. Aircraft, Equipment and Personnel.....	6
4.1. Flight Logistics.....	6
4.2. Aircraft and Equipment.....	7
4.2.1. Survey Aircraft.....	7
4.2.2. Electromagnetic System.....	7
4.2.3. Vtem®Plus System Specification.....	10
4.2.4. Airborne Magnetometer.....	10
4.2.5. Radar Altimeter.....	10
4.2.6. Digital Acquisition System.....	10
4.2.7. Base Station Magnetometer.....	11
4.2.8. Gps Ground Base Station.....	11
4.3. Personnel.....	11
5. Data Processing.....	12
5.1. Flight Path.....	12
5.2. Electromagnetic Data.....	12
5.3. Conductivity Depth Imaging (CDI).....	12
5.4. Anomaly Selection.....	12
5.5. Magnetic Microlevelling.....	13
5.6. Keating Correlation Coefficients.....	13
5.7. Geological Survey of Canada Data Levelling.....	14
5.7.1. Terminology.....	14
5.7.2. The Gsc Levelling Methodology.....	15
6. Final Products.....	18
6.1. Profile and Anomaly Databases.....	18
6.2. Gridded Data.....	18
6.3. Maps.....	19
6.4. Project Report.....	19
6.5. Flight Videos.....	19
7. Quality Assurance And Quality Control.....	19
7.1. Preproduction Calibration and Testing.....	20
7.2. Daily Calibrations and Preflight Precautions.....	20
7.3. Daily Field Quality Control.....	20
7.3.1. General.....	20
7.3.2. Electromagnetic Data.....	20

7.3.3. Magnetic Data and Magnetic Base Station	21
7.3.4. Altitude.....	21
7.4. Quality Control in the Office	21
8. References.....	22
Appendix A. Geophysical Data File Layout	23
Appendix B. Profile Archive Definition	24
Appendix C. EM Anomaly Archive Definition	26
Appendix D. Keating Correlation Archive Definition	27
Appendix E. Grid Archive Definition	28
Appendix F. Geotiff and Vector Archive Definition.....	29
Appendix G. Waveform and Conductivity Depth Image Archive Definition	30
Appendix H. Survey Block Co-ordinates.....	31
Appendix I. General Modeling Results of the VTEM System	32
Appendix J. EM Time Constant (Tau) Analysis	37
Appendix K. TEM Resistivity Depth Imaging (RDI).....	41
Appendix L. Test Sites and Calibrations	52

FIGURES

1. Survey area location map, Nestor Falls, Ontario.....	2
2. Flight path and magnetic base station (MAGBase) location displayed on Google Earth™ image.....	2
3. Digital elevation model (DEM) draped over a Google Earth™ image.....	3
4. Nestor Falls survey area, simplified bedrock geology with survey outline.....	6
5. VTEM current transmitter waveform.....	7
6. VTEM®Plus configuration with magnetometer	9
7. VTEM®Plus system configuration.....	9
8. EM anomaly symbols.....	13
9. Ontario Master Aeromagnetic Grid showing outline of the Vickers area sample data set to be levelled ...	16
10. Difference grid (difference between survey grid and master grid), Vickers survey.....	17
11. Difference grid after application of non-linear filtering and rotation, Vickers Survey	17
12. Level correction grid, Vickers survey	18
13. Data acquisition, data processing and interpretation workflow	22
I-1. vertical thin plate.....	33
I-2. inclined thin plate.....	33
I-3. inclined thin plate.....	33
I-4. horizontal thin plate	33
I-5. horizontal thick plate (linear scale of the response)	33
I-6. horizontal thick plate (log scale of the response).....	33
I-7. vertical thick plate (linear scale of the response). 50 m depth	34
I-8. vertical thick plate (log scale of the response). 50 m depth	34
I-9. vertical thick plate (linear scale of the response). 100 m depth	34

I-10. vertical thick plate (linear scale of the response). Depth/hor.thickness=2.5	34
I-11. horizontal thick plate (linear scale of the response)	34
I-12. horizontal thick plate (log scale of the response)	34
I-13. inclined long thick plate	35
I-14. two vertical thin plates	35
I-15. two horizontal thin plates	35
I-16. two vertical thick plates	35
I-17. Conductive vertical plate, depth 50 m, strike length 200 m, depth extend 150 m.....	36
J-1. Tau signals in the presence of good conductor and a poor conductor.....	37
J-2. Map of early time TAU. Area with overburden conductive layer and local sources	38
J-3. Map of full time range TAU with EM anomaly due to deep highly conductive target.....	38
J-4. dB/dt profile and RDI with different depths of targets.....	39
J-5. Map of total TAU and dB/dt profile.....	39
J-6. Typical dB/dt decays of VTEM data.....	40
K-1. Maxwell plate model and RDI from the calculated response for conductive “thin” plate (depth 50 m, dip 65 degree, depth extend 100 m)	41
K-2. Maxwell plate model and RDI from the calculated response for “thick” plate 18 m thickness, depth 50 m, depth extend 200 m).....	42
K-3. Maxwell plate model and RDI from the calculated response for bulk (“thick”) 100 m length, 40 m depth extend, 30 m thickness	43
K-4. Maxwell plate model and RDI from the calculated response for “thick” vertical target (depth 100 m, depth extend 100 m).....	43
K-5. Maxwell plate model and RDI from the calculated response for horizontal thin plate (depth 50 m, dim 50x100 m)	43
K-6. Maxwell plate model and RDI from the calculated response for horizontal thick (20 m) plate – less conductive (on the top), more conductive (below).....	44
K-7. Maxwell plate model and RDI from the calculated response for inclined thick (50 m) plate. Depth extends 150 m, depth to the target 50 m.....	45
K-8. Maxwell plate model and RDI from the calculated response for the long, wide and deep sub-horizontal plate (depth 140 m, dim 25x500x800 m) with conductive overburden.....	45
K-9. Maxwell plate models and RDIs from the calculated response for “thick” dipping plates (35, 50, 75 m thickness), depth 50 m, conductivity 2.5 S/m	46
K-10. Maxwell plate models and RDIs from the calculated response for “thick” (35 m thickness) dipping plate on different depth (50, 100, 150 m), conductivity 2.5 S/m	46
K-11. RDI section for the real horizontal and slightly dipping conductive layers.....	46
L-1. Bourget test lines on Google Earth™	52
L-2. Reid–Mahaffy test lines on Google Earth™	56
L-3. Plate test results performed on March 2, 2014.....	57
L-4. Radar altimeter test results performed on January 25, 2014	58
L-5. Flight path of Heading test performed on February 8, 2014	59
L-6. Flight path of Heading test performed on March 2, 2014	61

CREDITS

List of accountabilities and responsibilities:

- Jack Parker, Senior Manager, Earth Resources and Geoscience Mapping Section, Ontario Geological Survey (OGS), Ministry of Northern Development, Mines (MNDM) – accountable for the airborne geophysical survey projects, including contract management
- Edna Mueller-Markham, Senior Consulting Geophysicist, Paterson, Grant and Watson Limited (PGW), Toronto, Ontario, Geophysicist under contract to MNDM, responsible for the airborne geophysical survey project management, quality assurance (QA) and quality control (QC)
- Tom Watkins, Manager, Publication Services Unit, GeoServices Section, Ontario Geological Survey, MNDM – managed the project-related hard-copy products
- Desmond Rainsford, Geophysicist, Earth Resources and Geoscience Mapping Section, Ontario Geological Survey – responsible for final quality assurance (QA), quality control (QC) of published digital products
- Geotech Limited, Aurora, Ontario – data acquisition and data compilation.

DISCLAIMER

To enable the rapid dissemination of information, this digital data has not received a technical edit. However, every possible effort has been made to ensure the accuracy of the information presented in this report and the accompanying data; however, the Ontario Ministry of Northern Development and Mines does not assume liability for errors that may occur. Users should verify critical information.

CITATION

Parts of this publication may be quoted if credit is given. It is recommended that reference to this publication be made in the following form:

Ontario Geological Survey 2014. Ontario airborne geophysical surveys, magnetic and electromagnetic data, grid and profile data (ASCII and Geosoft® formats) and vector data, Nestor Falls area; Ontario Geological Survey, Geophysical Data Set 1076.

NOTE

Users of OGS products are encouraged to contact those Aboriginal communities whose traditional territories may be located in the mineral exploration area to discuss their project.

1. Introduction

This report describes a helicopter-borne combined aeromagnetic and electromagnetic survey carried out by Geotech Limited for the Ministry of Northern Development and Mines (MNDM) performed as part of the Ontario Geological Survey (OGS) geoscience program in the Nestor Falls area in northwestern Ontario.

The airborne survey contracts were awarded through a Request for Proposal and Contractor Selection process. The system and contractor selected for each survey area were judged on many criteria, including the following:

- applicability of the proposed system to the local geology and potential deposit types
- aircraft capabilities and safety plan
- experience with similar surveys
- QA/QC plan
- capacity to acquire the data and prepare final products in the allotted time
- price-performance.

2. SURVEY LOCATION AND SPECIFICATIONS

2.1. SURVEY LOCATION

Geotech Ltd. conducted a helicopter-borne geophysical survey over the Nestor Falls area in northwestern Ontario (Figures 1 and 2).

The geophysical surveys consisted of a combined helicopter-borne electromagnetic (EM) survey using the versatile time-domain electromagnetic (VTEM[®]Plus) system with Z-component measurements and an aeromagnetic survey using a cesium magnetometer. A total of 10 271 line-kilometres of geophysical data were acquired during the survey.

The crew was based out of Nestor Falls (*see* Figure 2) for the acquisition phase of the survey. The survey was flown between January 2 and March 1, 2014.

The survey area is located close to the town of Nestor Falls, Ontario. The outline of the survey area and the flight path layout is shown in Figure 2 below.



Figure 1. Survey area location map, Nestor Falls, Ontario.

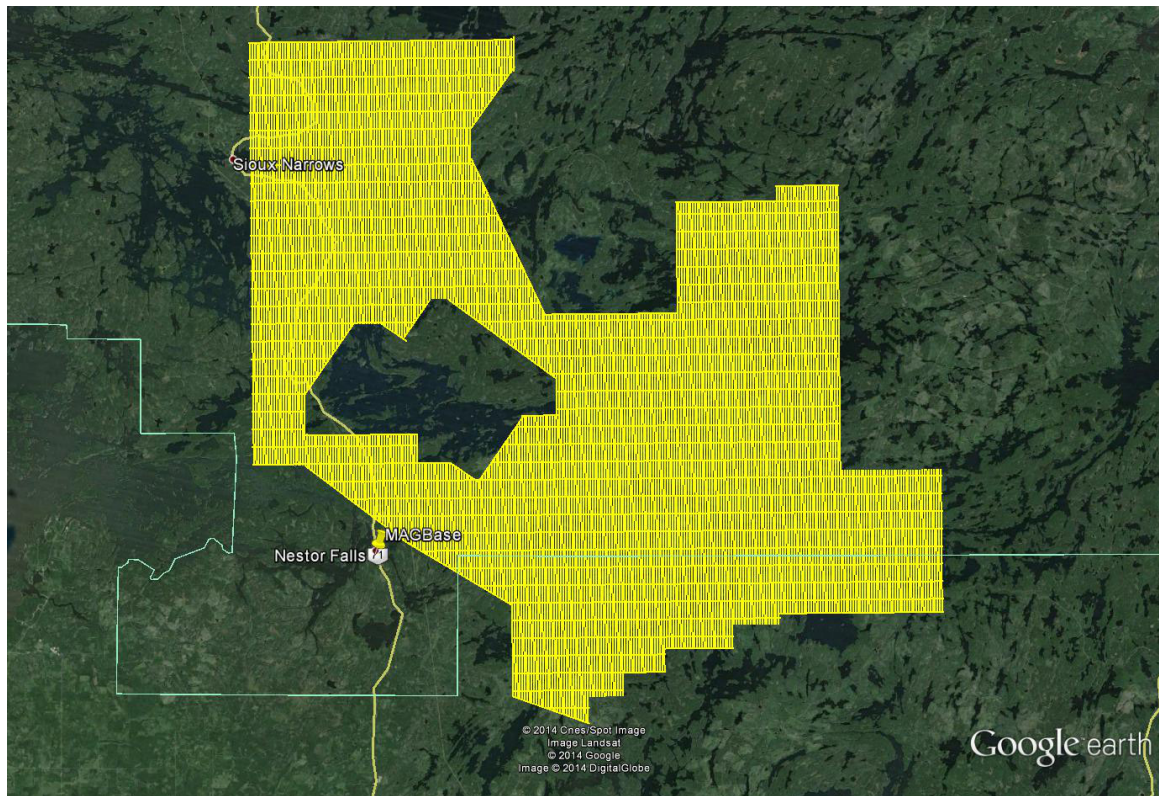


Figure 2. Flight path and magnetic base station (MAGBase) location displayed on Google Earth™ image.

2.2. TOPOGRAPHIC RELIEF AND CULTURAL FEATURES

Topographically, the block exhibits a shallow relief with an elevation ranging from 316 to 455 m above mean sea level (asl) over an area of 1785 km² (Figure 3).

The survey block comprises various rivers and streams running through the survey area which connect to lakes and wetlands. The most notable is Kakagi Lake located in the middle of the block. There are visible signs of culture, such as roads and towns, in the survey area.

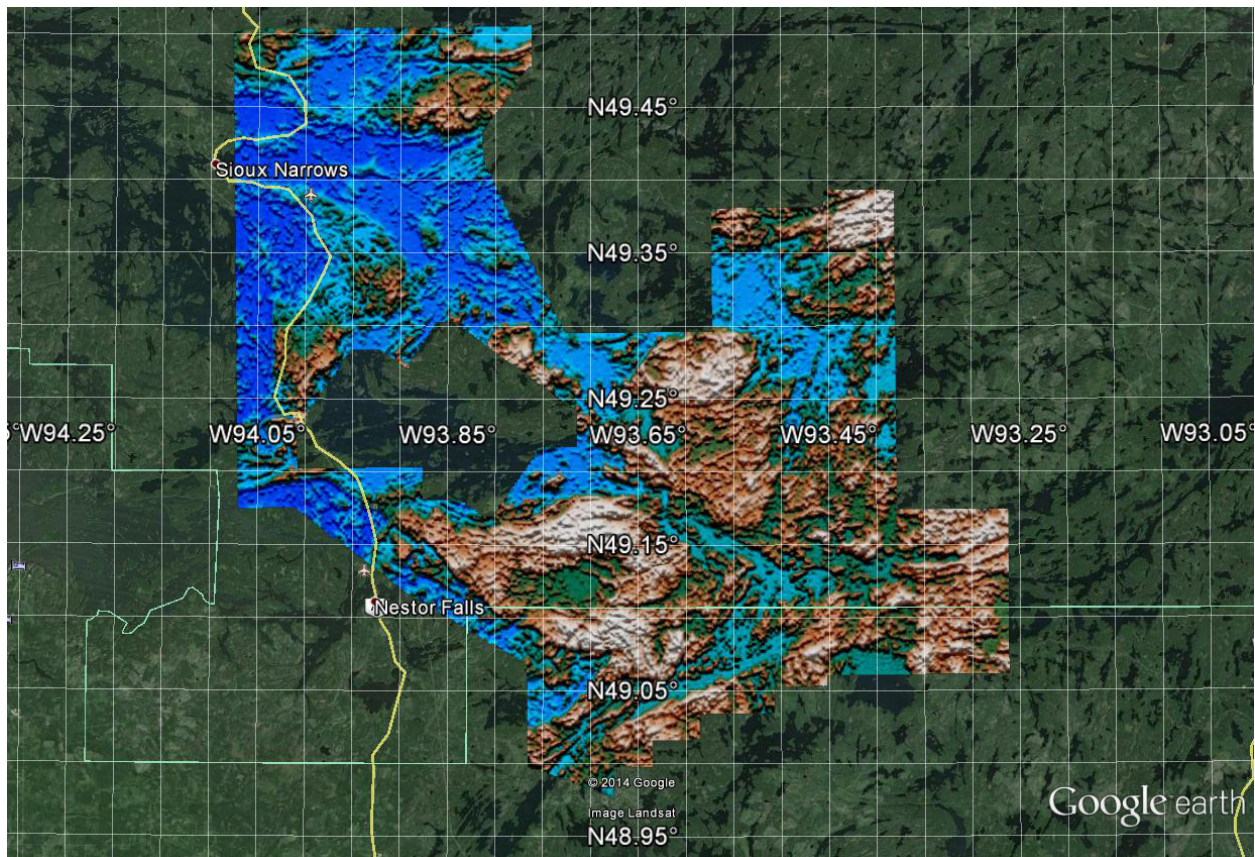


Figure 3. Digital elevation model (DEM) draped over a Google Earth™ Image. Elevation ranges from 316 to 455 m asl.

2.3. SURVEY AND SYSTEM SPECIFICATIONS

Data quality control and quality assurance, and preliminary data processing were carried out on a daily basis during the acquisition phase of the project. Final data processing followed immediately after completion of the survey. Final reporting, data presentation and archiving were completed at Geotech's Aurora office in June 2014.

The survey block was flown in a south to north (N 0° E azimuth) direction, with traverse line spacing of 200 m as depicted in Figure 4. Tie-lines were flown perpendicular to the traverse lines (N 90° E azimuth) at a spacing of 1500 m. For more detailed information on the flight spacing and direction see Table 1.

2.4. DATA ACQUISITION

2.4.1. FLIGHT LINE SPECIFICATIONS

The survey block (see Figure 2) and general flight specifications are as follows:

Table 1. Flight line specifications

Survey block	Traverse Line spacing (m)	Area (km ²)	Planned ¹ Line-km	Actual Line-km	Flight direction	Line numbers
Nestor Falls	Traverse: 200	1785	8925.1	9069.9	N 0° E / N 180° E	L310 – L3250
	Tie: 1500		1345.9	1360.4	N 90° E / N 270° E	T4000 – T5180
TOTAL		1785	10271	10430.3		

Survey block boundary co-ordinates are provided in Appendix H.

2.4.2. SURVEY OPERATIONS

Survey operations were based out of Nestor Falls, Ontario from January 2 to March 1, 2014. The flight schedule for the survey is outlined in Table 2 below.

Table 2. Survey flight schedule

Date	Flight #	Flown km	Block	Crew location	Comments
2-Jan-2014				Timmins, ON	Testing lines flown from Jan 2 to 21, 2014
22-Jan-2014				Nestor Falls, ON	Mobilization
23-Jan-2014				Nestor Falls, ON	Crew arrived
24-Jan-2014				Nestor Falls, ON	System assembly
25-Jan-2014				Nestor Falls, ON	Test flight
26-Jan-2014	1	72	NF	Nestor Falls, ON	72 km flown waiting on client approval
27-Jan-2014	2,3	397	NF	Nestor Falls, ON	397 km flown
28-Jan-2014	4,5,6	421	NF	Nestor Falls, ON	421 km flown
29-Jan-2014				Nestor Falls, ON	No production due to technical issues
30-Jan-2014				Nestor Falls, ON	No production due to technical issues
31-Jan-2014				Nestor Falls, ON	Testing completed
1-Feb-2014	7,8,9	560	NF	Nestor Falls, ON	560 km flown
2-Feb-2014	10,11	417	NF	Nestor Falls, ON	417 km flown
3-Feb-2014	12,13,14	599	NF	Nestor Falls, ON	599 km flown
4-Feb-2014	15,16	446	NF	Nestor Falls, ON	446 km flown
5-Feb-2014	17	153	NF	Nestor Falls, ON	15 3km flown
6-Feb-2014	18,19,20	469	NF	Nestor Falls, ON	469 km flown
7-Feb-2014	21,22,23	569	NF	Nestor Falls, ON	569 km flown
8-Feb-2014	24,25	262	NF	Nestor Falls, ON	262 km flown
9-Feb-2014	26,27,28	601	NF	Nestor Falls, ON	601 km flown
10-Feb-2014	29,30,31	559	NF	Nestor Falls, ON	559 km flown
11-Feb-2014	32,33	332	NF	Nestor Falls, ON	332 km flown

¹ Note: Actual line-kilometres represent the total line-kilometres in the final database. These line-kilometres normally exceed the planned line-kilometres, as indicated in the survey NAV files.

Date	Flight #	Flown km	Block	Crew location	Comments
12-Feb-2014	34,35,36	495	NF	Nestor Falls, ON	495 km flown
13-Feb-2014	37	188	NF	Nestor Falls, ON	188 km flown, limited due to weather
14-Feb-2014	38,39,40	391	NF	Nestor Falls, ON	391 km flown
15-Feb-2014	41	144	NF	Nestor Falls, ON	144 km flown
16-Feb-2014	42,43	362	NF	Nestor Falls, ON	362 km flown
17-Feb-2014				Nestor Falls, ON	No production due to weather
18-Feb-2014	44,45,46	497	NF	Nestor Falls, ON	497 km flown
19-Feb-2014	47,48	114	NF	Nestor Falls, ON	114 km flown
20-Feb-2014				Nestor Falls, ON	No production due to weather
21-Feb-2014				Nestor Falls, ON	No production due to weather
22-Feb-2014	49,50	313	NF	Nestor Falls, ON	313 km flown
23-Feb-2014				Nestor Falls, ON	No production due to weather
24-Feb-2014	51,52	422	NF	Nestor Falls, ON	422 km flown
25-Feb-2014	53,54	416	NF	Nestor Falls, ON	416km flown
26-Feb-2014				Nestor Falls, ON	No production due to weather
27-Feb-2014	55,56	433	NF	Nestor Falls, ON	433 km flown
28-Feb-2014	57,58	417	NF	Nestor Falls, ON	417 km flown
1-Mar-2014	59,60,61	388	NF	Nestor Falls, ON	Remaining kms were flown –flying complete

3. Survey Area Geology

The following description of the regional geology of the area (Figure 4) is drawn from Lewis and Woolgar (2011). The area is underlain by Archean rocks of the western Wabigoon subprovince. The rocks consist primarily of mafic, intermediate and felsic metavolcanic rocks with minor metasedimentary rocks, and are intruded by various mafic to felsic plutonic rocks. In the subsequent description, the “meta” prefix is omitted for the sake of brevity. The volcanic rocks are divisible into 2 distinct sequences: the Rowan Lake volcanic rocks consisting predominantly of mafic volcanic rocks and the Cameron Lake volcanic rocks that exhibit greater compositional diversity. All observed facing indicators suggest that the Cameron Lake volcanic rocks are younger than the Rowan Lake volcanic rocks.

Major structures in the area include the Monte Cristo fault and the Shingwak Lake anticline. The northeast-trending Monte Cristo fault merges with the southeast-trending Pipestone–Cameron, a major, regional-scale structure that can be traced for over 100 km. The structural facing in the Shingwak Lake anticline is toward the southwest.

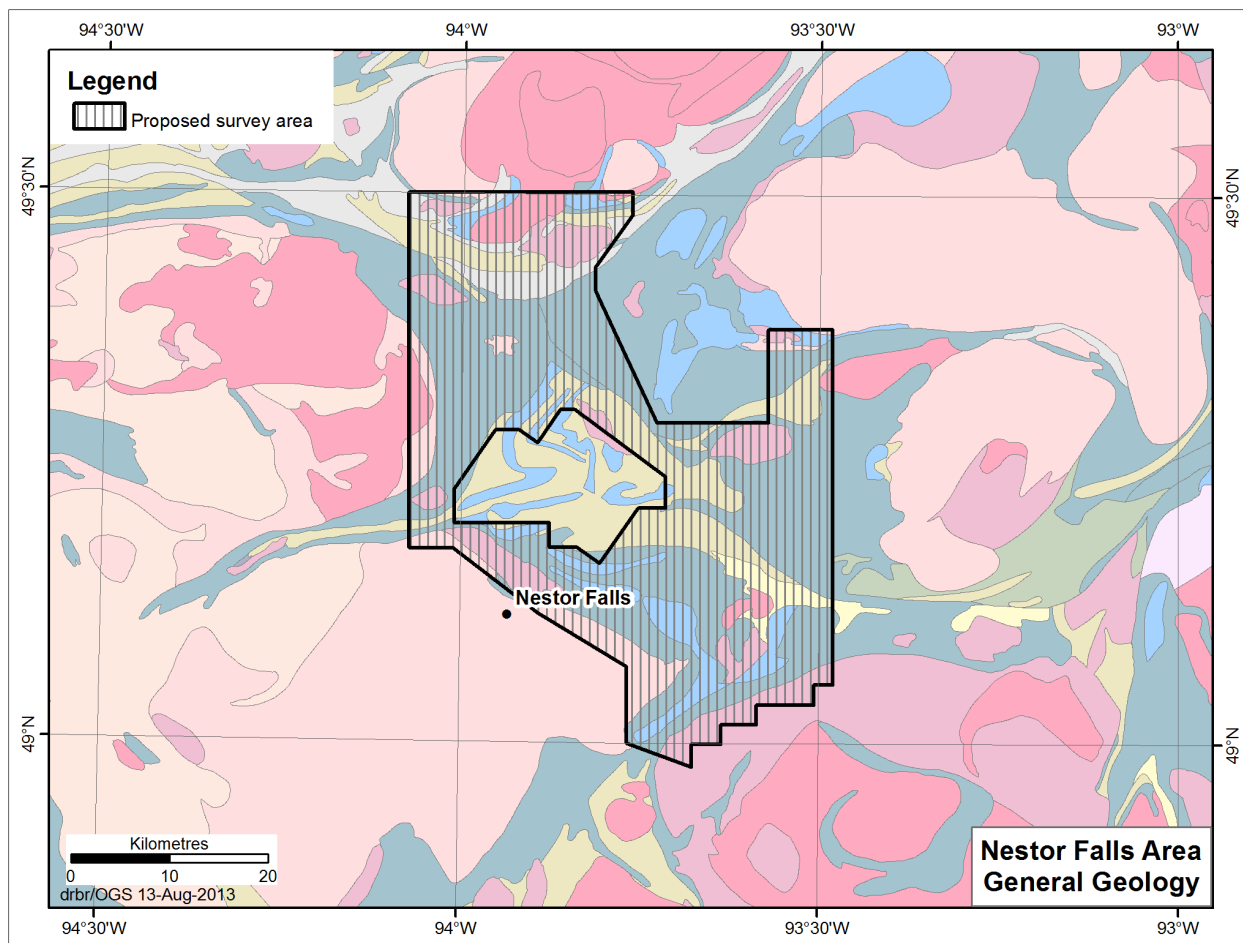


Figure 4. Nestor Falls survey area, simplified bedrock geology with survey outline (geology after Ontario Geological Survey, 2011).

4. AIRCRAFT, EQUIPMENT AND PERSONNEL

4.1. FLIGHT LOGISTICS

During the survey the helicopter was maintained at a mean altitude of 92 m above the ground with an average survey speed of 80 km/hour. This allowed for an average EM bird terrain clearance of 45 m and a magnetic sensor clearance of 59 m.

The on board operator was responsible for monitoring the system integrity. He also maintained a detailed flight log during the survey, tracking the times of the flight as well as any unusual geophysical or topographic features.

Upon return to base camp, the survey data was transferred from a compact flash card (PCMCIA) to the data processing computer. The data were then uploaded via ftp to the Geotech office in Aurora for daily quality assurance and quality control by qualified personnel.

4.2. AIRCRAFT AND EQUIPMENT

4.2.1. SURVEY AIRCRAFT

The survey was flown using a Eurocopter Aerospatiale (Astar) 350 B3 helicopter, registration C-FK0I. The helicopter is owned and operated by Geotech Aviation. Installation of the geophysical and ancillary equipment was carried out by Geotech Ltd crew.

4.2.2. ELECTROMAGNETIC SYSTEM

The electromagnetic equipment, used for the survey, was a Geotech Time Domain EM VTEM[®]Plus system (serial number 20). The configuration is as indicated in Figures 6 and 7.

The VTEM[®]Plus receiver and transmitter coils were in a concentric-coplanar and Z-direction oriented configuration. The transmitter current waveform is shown in Figure 5.

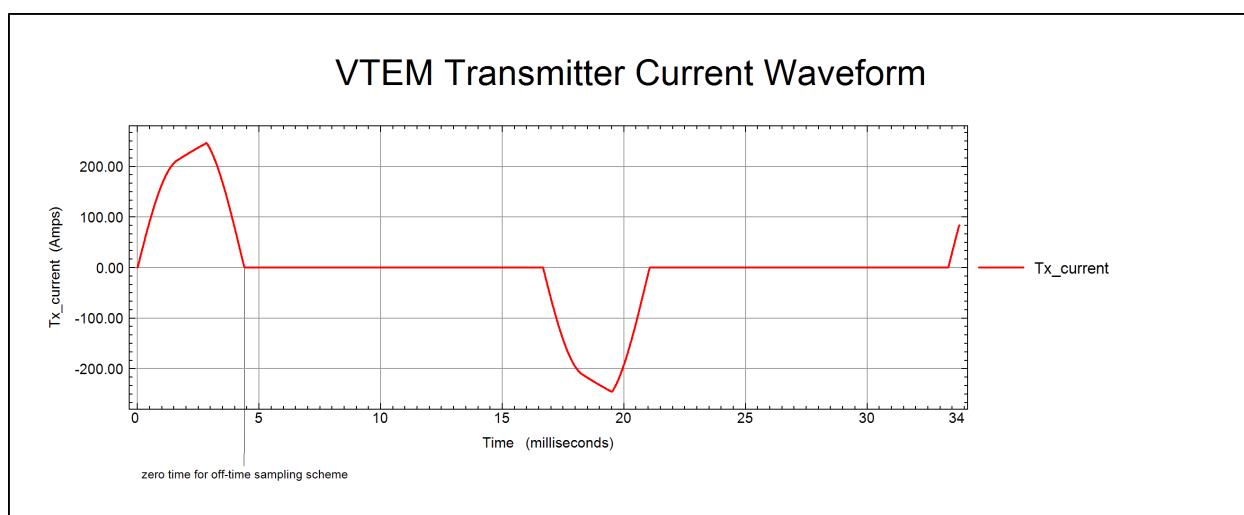


Figure 5. VTEM current transmitter waveform.

The VTEM decay sampling scheme is shown in Table 3 below. Thirty-two time measurement gates were used for the final data processing in the range from 0.096 to 7.036 msec. Zero time for the off-time sampling scheme is equal to the current pulse width and is defined as the time near the end of the turn-off ramp where the dI/dt (current/time, *see* Figure 5) waveform falls to 1/2 of its peak value.

Table 3. Off-time decay sampling scheme

VTEM Decay Sampling Scheme				
index	Start	End	Middle	Width
milliseconds				
14	0.090	0.103	0.096	0.013
15	0.103	0.118	0.110	0.015
16	0.118	0.136	0.126	0.018
17	0.136	0.156	0.145	0.020
18	0.156	0.179	0.167	0.023
19	0.179	0.206	0.192	0.027
20	0.206	0.236	0.220	0.030
21	0.236	0.271	0.253	0.035

VTEM Decay Sampling Scheme				
index	Start	End	Middle	Width
milliseconds				
22	0.271	0.312	0.290	0.040
23	0.312	0.358	0.333	0.046
24	0.358	0.411	0.383	0.053
25	0.411	0.472	0.440	0.061
26	0.472	0.543	0.505	0.070
27	0.543	0.623	0.580	0.081
28	0.623	0.716	0.667	0.093
29	0.716	0.823	0.766	0.107
30	0.823	0.945	0.880	0.122
31	0.945	1.086	1.010	0.141
32	1.086	1.247	1.161	0.161
33	1.247	1.432	1.333	0.185
34	1.432	1.646	1.531	0.214
35	1.646	1.891	1.760	0.245
36	1.891	2.172	2.021	0.281
37	2.172	2.495	2.323	0.323
38	2.495	2.865	2.667	0.370
39	2.865	3.292	3.063	0.427
40	3.292	3.781	3.521	0.490
41	3.781	4.341	4.042	0.560
42	4.341	4.987	4.641	0.646
43	4.987	5.729	5.333	0.742
44	5.729	6.581	6.125	0.852
45	6.581	7.560	7.036	0.979

The EM bird was towed at a mean distance of 47 m below the aircraft as shown in Figures 6 and 7.

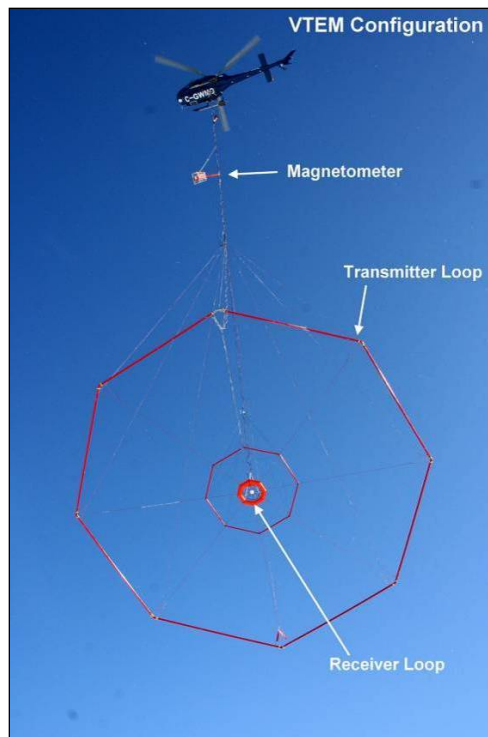


Figure 6. VTEM[®]Plus configuration, with magnetometer.

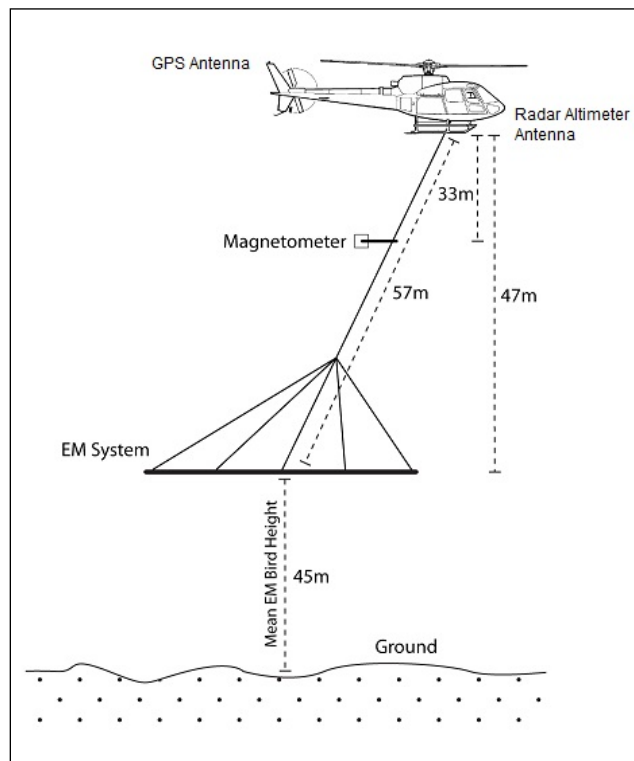


Figure 7. VTEM[®]Plus system configuration (not to scale).

4.2.3. VTEM[®] PLUS SYSTEM SPECIFICATION

Transmitter

- Transmitter loop diameter: 26 m
- Effective transmitter loop area: 2123.7 m²
- Number of turns: 4
- Transmitter base frequency: 30 Hz
- Peak current: 246 A
- Pulse width: 4.40 ms
- Wave form shape: trapezoid
- Peak dipole moment (NIA): 522 430 Am²
- Actual average EM Bird terrain clearance: 45 m above the ground

Receiver

- Z-Coil diameter: 1.2 m
- Number of turns: 100
- Effective coil area: 113.04 m²

4.2.4. AIRBORNE MAGNETOMETER

The magnetic sensor utilized for the survey was a Geometrics[®] Model G823A optically pumped cesium-vapour magnetic field sensor mounted 33 m below the helicopter, as shown in Figure 7. The sensitivity of the magnetic sensor is 0.02 nanoTesla (nT) at a sampling interval of 0.1 seconds.

4.2.5. RADAR ALTIMETER

A Terra TRA 3000/TRI 40 radar altimeter was used to record terrain clearance. The antenna was mounted beneath the bubble of the helicopter cockpit (Figure 7).

4.2.6. DIGITAL ACQUISITION SYSTEM

A Geotech data acquisition system recorded the digital survey data on an internal compact flash card. Data are displayed on an LCD screen as traces to allow the operator to monitor the integrity of the system. The data type and sampling interval as provided in Table 4.

Table 4. Acquisition sampling rates

Data Type	Sampling
TDEM	0.1 sec
Magnetometer	0.1 sec
GPS Position	0.2 sec
Radar Altimeter	0.2 sec

4.2.7. BASE STATION MAGNETOMETER

A dedicated computer including high sensitivity base station cesium magnetometer and a GPS system to record the GPS time together with the magnetic data was employed to record magnetic activity. The magnetometer had a sensitivity of better than 0.01 nT at a sampling interval of 0.1 s. Digital data from the base station magnetometer were recorded at all times during the survey. The digital data included the date, an absolute magnetic value, and GPS time with accurate synchronization to the aircraft data acquisition system. A Geometrics® G822B high-sensitivity, cesium-vapour magnetometer and integrated GPS unit for the accurate time synchronization was used with 10 Hz data output.

The base station magnetometer sensor was installed on a hill South-west of the motel (49°06.4785' N, 93°55.6014' W); away from electric transmission lines and moving metal (iron) objects such as motor vehicles. The base station data were backed-up to the data processing computer at the end of each survey day.

4.2.8. GPS GROUND BASE STATION

A dedicated Novatel® ProPak™-V3 TR20 GPS receiver and ground-based GPS antenna was used with a 10 Hz Raw GPS data recording. Postflight differential GPS data processing utilizing Novatel® GrafNav 8.3 software was used to produce sub-meter accuracy of the airborne system location at 10 Hz sampling interval.

4.3. PERSONNEL

The following personnel were involved with the survey.

Field

Project Manager:	Darren Tuck (Office)
Data QC:	Neil Fiset (Office)
Crew chief:	Colin Lennox
Operator:	Paul Taylor
Pilot:	Walter Zec Brad MacRae
Mechanical Engineer:	Dylan Pike Darren Patterson

The survey pilot and the mechanical engineer were employed directly by the helicopter operator – Geotech Aviation.

Office

Preliminary Data Processing:	Neil Fiset
Interim Data Processor:	Shaolin Lu Marta Orta
Supervisor of Data QC:	Geoffrey Plastow
Reporting/Mapping:	Wendy Acorn

The data acquisition phase was carried out under the supervision of Andrei Bagrianski, *P. Geo.*, Chief Operating Officer. The processing and interpretation phase was under the supervision of Geoffrey Plastow, *P. Geo.* Customer relations were looked after by David Hitz.

5. DATA PROCESSING

Data compilation and processing were carried out using Geosoft® OASIS montaj™ and programs proprietary to Geotech Ltd.

5.1. FLIGHT PATH

The flight path, recorded by the data acquisition program as WGS 84 latitude/longitude datum and co-ordinate system, was converted to NAD83, UTM Zone 15 North co-ordinate system in Oasis montaj™.

The flight path was drawn using linear interpolation between x, y positions from the navigation system. Positions are updated every second and expressed as UTM easting (x) and UTM northing (y).

5.2. ELECTROMAGNETIC DATA

A three-stage digital filtering process was used to reject major sferic events and to reduce system noise. Local sferic activity can produce sharp, large-amplitude events that cannot be removed by conventional filtering procedures. Smoothing or stacking will reduce their amplitude but leave a broader residual response that can be confused with geological phenomena. To avoid this possibility, a computer algorithm searches out and rejects the major sferic events.

The signal to noise ratio was further improved by the application of a low pass linear digital filter. This filter has zero phase-shift which prevents any lag or peak displacement from occurring, and it suppresses only variations with a wavelength less than about 1 second or 25 m. A symmetrical, 1 second linear filter was used.

The Z-axis receiver coil was oriented parallel to the transmitter coil axis and both were horizontal to the ground. Generalized modeling results of the VTEM system are shown in Appendix I.

Z-component data produce double peak type anomalies for “thin” sub vertical targets and single peak anomalies for “thick” targets. The limits and changeover of “thin-thick” depends on dimensions of the TEM system (Appendix I, Figure I-17).

5.3. CONDUCTIVITY DEPTH IMAGING (CDI)

Five hundred and one (501) apparent conductivity-depth images (CDI) were generated for all survey lines (traverse and tie-lines), calculated from dBz/dt response. CDIs, presented in mS/m, were obtained from the apparent resistivity transformation algorithm explained in Appendix K.

Apparent conductivity depth-slices, extracted from the 3D voxel, are provided every 100 m for 4 levels of depth below ground level (0 m, -100 m, -200 m and -300 m).

5.4. ANOMALY SELECTION

The EM data were subjected to an anomaly recognition process using all the channels of the dBz/dt profiles. The resulting EM anomaly picks are presented as overlays on the maps and correspond to the approximate position of the conductors' centres projected to surface.

Each individual conductor pick is represented by an anomaly symbol classified according to the calculated conductance². Identified anomalies were classified into one of six categories, as presented in

² Note: Conductance values were obtained from the dB/dt and B-Field EM time constants (Tau) whose relationships to Tau were calculated using the oblate spheroid model of McNeill (1980).

Figure 8. The anomaly symbol is accompanied by postings denoting the dBz/dt conductance (upper-right) calculated from the time-constant (τ)³, and the identification of the anomaly (upper left), a unique number to each flight line.

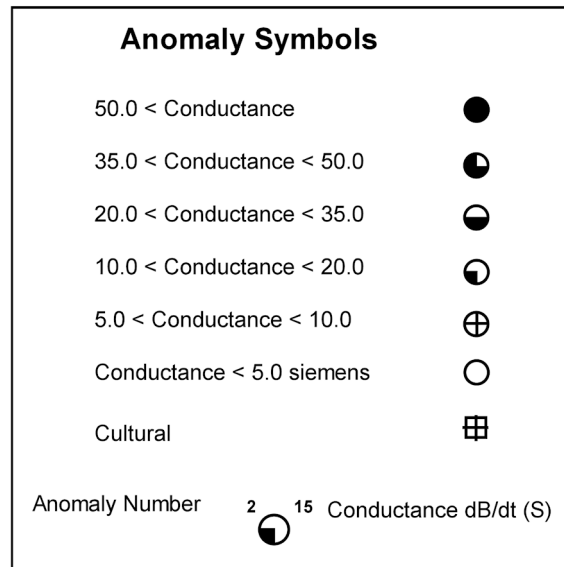


Figure 8. EM anomaly symbols.

The anomalous responses have been picked, reviewed and edited by an interpreter on a line-by-line basis to discriminate between bedrock, overburden and culture conductors. The accepted channels are provided in a Geosoft database.

5.5. MAGNETIC MICROLEVELLING

Microlevelling is the process of removing residual flight line noise that remains after conventional levelling using control lines. It has become increasingly important as the resolution of aeromagnetic surveys has improved and the requirement of interpreting subtle geophysical anomalies has increased.

To isolate and remove this noise, the following procedure was employed. An elliptical reject filter, aligned with the flight lines, was first applied to the levelled total magnetic field grid. This filter removes features with a long wavelength in the flight line direction, but a short wavelength in the transverse direction. While removing the unwanted residual levelling errors, it also significantly distorts higher amplitude anomalies.

In order to minimize the effect on real anomalies, the flight path was ‘threaded’ through the filtered grid and a database profile channel was created from the grid. The difference between the control line levelled magnetic profile and this filtered profile was calculated. The difference profile was clipped to the amplitude of the observed noise in the grid. A half cosine roll-off filter was then applied to this channel and a final correction profile was derived with wavelengths longer than 1 kilometre. This microlevel correction profile was applied to the levelled magnetic profile and a final magnetic profile channel was created.

5.6. KEATING CORRELATION COEFFICIENTS

Possible kimberlite targets are recognized from the residual magnetic intensity data, based on the identification of roughly circular anomalies. This procedure is automated by using a known pattern

³ An explanation of the EM time constant (τ) approach to VTEM data is provided in Appendix E.

recognition technique (Keating 1995), which consists of computing, over a moving window, a first-order regression between a vertical cylinder model anomaly and the gridded magnetic data. Only the results, where the absolute value of the correlation coefficient is above a threshold of 75%, were retained. On the magnetic maps, the results are depicted as circular symbols, scaled to reflect the correlation value. The most favourable targets are those that exhibit a cluster of high amplitude solutions. Correlation coefficients with a negative value correspond to reversely magnetized sources.

The cylinder model parameters are as follows:

- Cylinder diameter: 200 m
- Cylinder length: infinite
- Overburden thickness: 8.1 m
- Magnetic inclination: 74° N
- Magnetic declination: 0.28° W
- Magnetization scale factor: 100
- Model window size: 13 x 13 cells (520 m x 520 m)
- Model window grid cell size: 40 m

It is important to be aware that other magnetic sources may correlate well with the vertical cylinder model, whereas some kimberlite pipes of irregular geometry may not. The user should study the magnetic anomaly that corresponds with the Keating symbols, to determine whether it does resemble a kimberlite pipe signature, reflects some other type of source or even noise in the data e.g., boudinage (beading) effect of the bi-cubic spline gridding. All available geological information should be incorporated into kimberlite pipe target selection.

5.7. GEOLOGICAL SURVEY OF CANADA DATA LEVELLING

In 1989, as part of the requirements for the contract with the Ontario Geological Survey (OGS) to compile and level all existing Geological Survey of Canada (GSC) aeromagnetic data (flown prior to 1989) in Ontario, PGW developed a robust method to level the magnetic data of various base levels to a common datum provided by the GSC as 812.8 m grids. The essential theoretical aspects of the levelling methodology were fully discussed in Gupta et al. (1989), and Reford et al. (1990). The method was later applied to the remainder of the GSC data across Canada and the high-resolution, combined aeromagnetic and EM (AMEM) surveys flown by the OGS. It has since been applied to all newly acquired OGS aeromagnetic surveys.

5.7.1. TERMINOLOGY

The Master grid refers to the 200 m Ontario magnetic grid compiled and levelled to the 812.8 m magnetic datum from the Geological Survey of Canada.

GSC levelling is the process of levelling profile data to a master grid, first applied to GSC data.

Intrasurvey levelling or microlevelling refers to the removal of residual line noise described earlier in this chapter; the wavelengths of the noise removed are usually shorter than tie line spacing.

Intersurvey levelling or GSC levelling refers to the level adjustments applied to a block of data; the adjustments are the long wavelength (in the order of tens of kilometres) differences with respect to a common datum, in this case, the 200 m Ontario master grid, which was derived from all pre-1989 GSC magnetic data and adjusted, in turn, by the 812.8 m GSC Canada wide grid.

5.7.2. THE GSC LEVELLING METHODOLOGY

The GSC levelling methodology is described below, using the Vickers survey flown for OGS as an example.

Several data processing procedures are assumed to be applied to the survey data prior to levelling, such as microlevelling, IGRF calculation and removal. The final levelled data are gridded at 1/5 of the line spacing. If a survey was flown as several distinct blocks with different flight directions, then each block is treated as an independent survey.

The steps in the GSC levelling process are as follows:

1. Create an upward continuation of the survey grid to 305 m

Almost all recent surveys (1990 and later) to be compiled were flown at a nominal terrain clearance of 100 m or less. The first step in the levelling method is to upward continue the survey grid to 305 m, the nominal terrain clearance of the Ontario Master Grid (Figure 9). The grid cell size for the survey grids is set at 100 m. Since the wavelengths of level corrections will be greater than 10 to 15 km, working with 100 m or even 200 m grids at this stage will not affect the integrity of the levelling method. Only at the very end, when the level corrections are imported into the databases, will the level correction grids be re-gridded to 1/5 of line spacing.

The unlevelled 100 m grid is extended by at least 2 grid cells beyond the actual survey boundary, so that, in the subsequent processing, all data points are covered.

2. Create a difference grid between the survey grid and the Ontario master grid.

The difference between the upward continued survey grid and the Ontario master grid, re-gridded at 100 m, is computed (Figure 10). The short wavelengths represent the higher resolution of the survey grid. The long wavelengths represent the level difference between the two grids.

3. Rotate difference grid so that flight line direction is parallel with grid column or row, if necessary.
4. Apply the first pass of a non-linear filter (Naudy and Dreyer 1968) of wavelength on the order of 15 to 20 km along the flight line direction. Reapply the same non-linear filter across the flight line direction.
5. Apply the second pass of a non-linear filter of wavelength on the order of 2000 to 5000 m along the flight line direction. Reapply the same non-linear filter across the flight line direction.
6. Rotate the filtered grid back to its original (true) orientation (Figure 11).
7. Apply a low pass filter to the non-linear filtered grid.

Streaks may remain in the non-linear filtered grid, mostly caused by edge effects. They must be removed by a frequency-domain, low pass filter with the wavelengths in the order of 25 km (Figure 12).

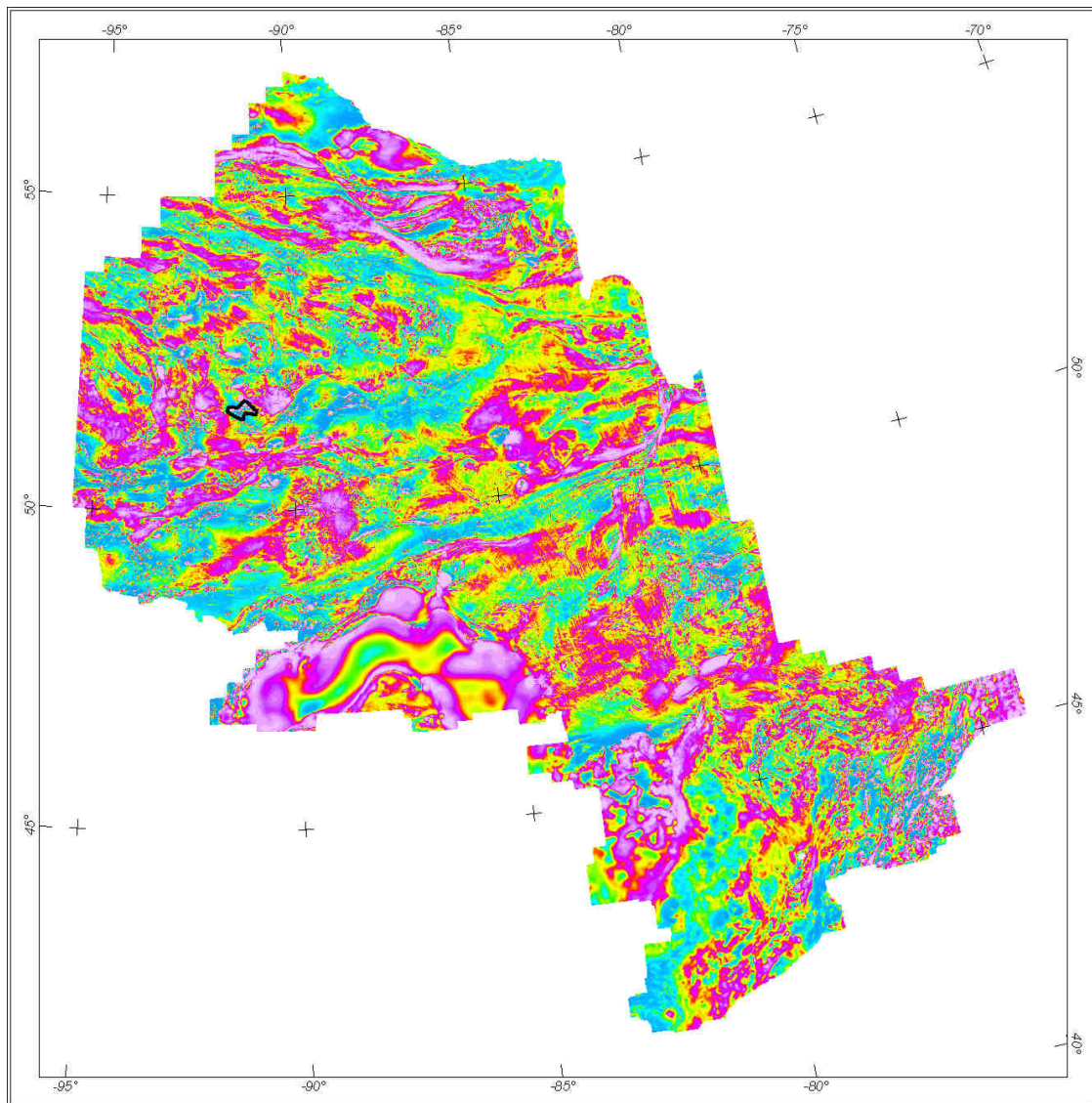


Figure 9. The Ontario Master Aeromagnetic Grid (Ontario Geological Survey 1999). The outline for the sample data set to be levelled (Vickers) is shown.

8. Re-grid to 1/5 line spacing and import level corrections into database.
9. Subtract the level correction channel from the un-levelled channel to obtain the level corrected channel.
10. Make final grid using the gridding algorithm of choice with grid cell size at 1/5 of line spacing.

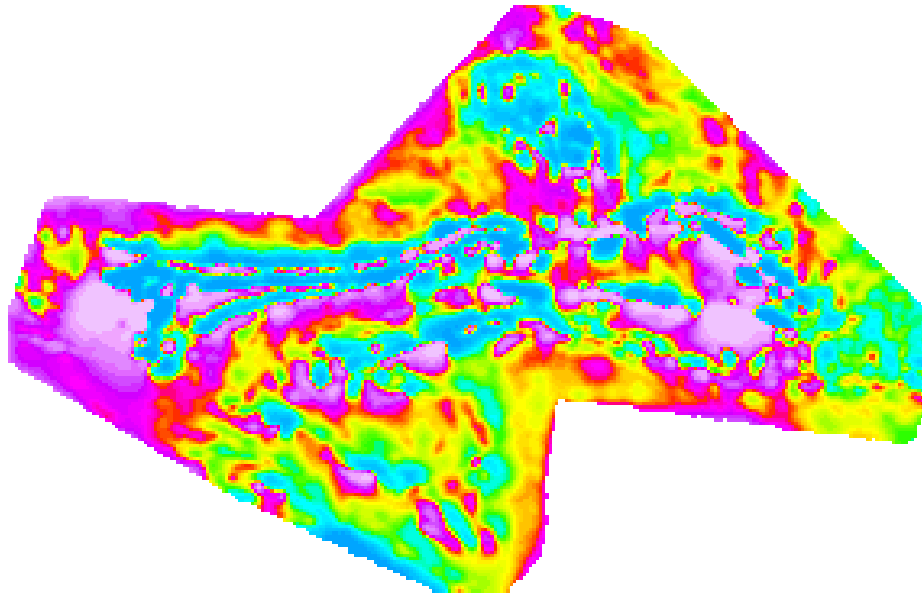


Figure 10. Difference grid (difference between survey grid and master grid), Vickers survey (Ontario Geological Survey 2002).

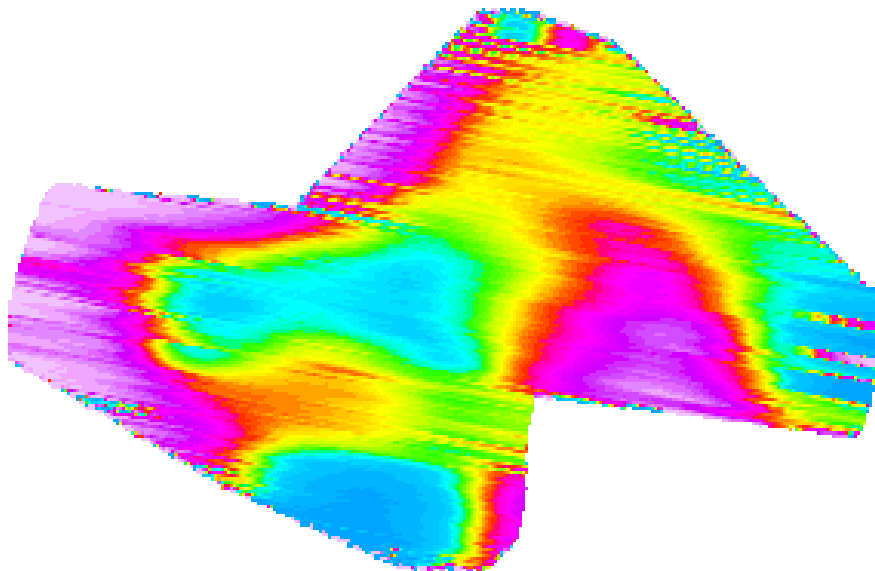


Figure 11. Difference grid after application of non-linear filtering and rotation, Vickers Survey.

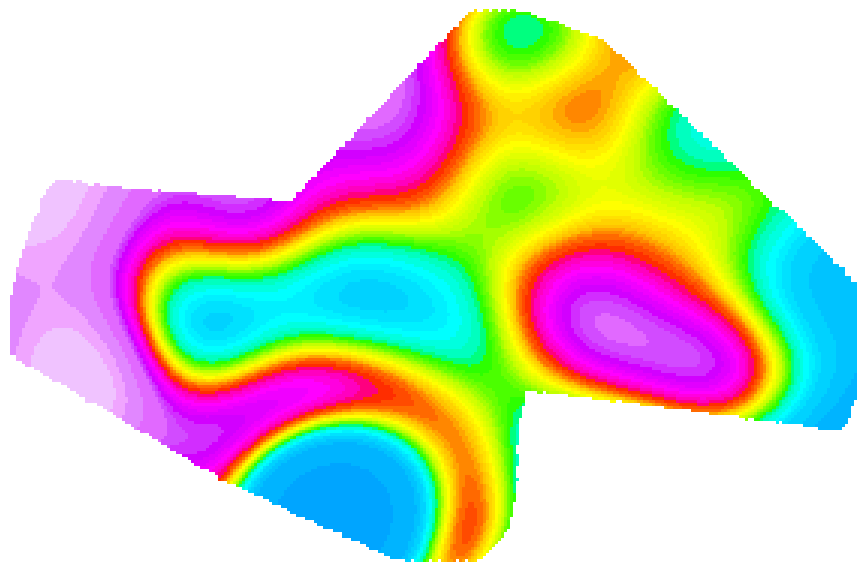


Figure 12. Level correction grid, Vickers survey.

Survey Specific Parameters

The following GSC levelling parameters were used in the Nestor Falls survey:

Upward continue 246 m to 305 m

- OGS 200 m grid regridded to 100 m (Ontario-wide TMI grid)
- Difference grid filtered with regrid.gx using LP=7000, 7000, 1750, 1750
- Magmap filtered with LP=10000
- Sampled back to database (lev_corr)
- Correction subtracted from residual magnetic intensity channel

6. FINAL PRODUCTS

The following products were delivered to MNDM.

6.1. PROFILE AND ANOMALY DATABASES

The following databases are provided in both Geosoft® GDB and ASCII format.

- Magnetic and electromagnetic profile database
- EM anomaly database
- Keating correlation coefficient database

6.2. GRIDDED DATA

The following data, gridded from co-ordinates in UTM Zone 15N, NAD83 datum, are provided in both Geosoft® GRD and GXF formats.

- digital elevation model
- GSC levelled residual magnetic field

- calculated second vertical derivative of the GSC levelled residual magnetic field
- TDEM decay constant Z-component
- apparent conductivity depth slices

6.3. MAPS

Final maps were produced at a scale of 1:20 000 and 1:50 000 for best representation of the survey size and line spacing. The co-ordinate and/or projection system used was NAD83 Datum, UTM Zone 15 North. The following maps were created.

- GSC levelled residual magnetic field with EM anomalies and Keating correlation coefficients
- GSC levelled residual magnetic field contours with EM anomalies
- shaded second vertical derivative and Keating coefficients
- TDEM decay constant with EM anomalies
- TDEM apparent conductivity with EM anomalies

Digital 1:20 000 scale maps in Geosoft® MAP format, with a topographic layer, of the following:

- residual magnetic field contours with electromagnetic anomalies and Keating coefficients, maps 82 634 to 82 642 (inclusive)

Digital 1:50 000 scale maps in Geosoft® MAP format, with a topographic layer, of the following:

- colour-filled contours of the residual magnetic field and electromagnetic anomalies, maps 82 643 and 82 644
- shaded colour image of the second vertical derivative of the residual magnetic field and Keating coefficients, maps 82 645 and 82 646
- colour-filled contours of the EM decay constant and electromagnetic anomalies, maps 82 647 and 82 648
- colour-filled contours of the apparent conductance and electromagnetic anomalies, maps 82 649 and 82 650

6.4. PROJECT REPORT

The survey report describes the data acquisition, processing, and final presentation of the survey results. The survey report is provided only digitally, in portable document format (*.pdf*).

6.5. FLIGHT VIDEOS

The digitally recorded video from each survey flight are provided in a compressed binary format on an external disc drive.

7. QUALITY ASSURANCE AND QUALITY CONTROL

Quality assurance and quality control (QA/QC) were undertaken by the survey contractor, Geotech Ltd., PGW (QA/QC Geophysicist), and MNDM. Stringent QA/QC was emphasized throughout the project so that the optimal geological signal was measured, archived and presented. The quality control procedures are summarized below.

7.1. PREPRODUCTION CALIBRATION AND TESTING

Test surveys were flown at the Bourget and Reid–Mahaffy test sites to calibrate the magnetometer and TDEM systems respectively. These tests are presented in Appendix L

In addition the following tests were carried out on the survey site:

1. Polarity Test – performed prior to the survey commencing. This test was designed to ensure that the polarity of the system is correct.
2. Aluminium Plate Test – performed prior to the survey commencing and at the end of every week. The test checked the sensitivity of the system during the survey period and ensured that the system was calibrated properly at all times.
3. Radar Altimeter Test – performed prior to survey commencing or if a new radar altimeter was installed. The test was performed to ensure the accuracy of the radar altimeter.

7.2. DAILY CALIBRATIONS AND PREFLIGHT PRECAUTIONS

The TDEM system and magnetometer were sufficiently warmed up before each survey day to minimize temperature-related system drifting.

- Timing and synchronization of all recording instruments was checked for correct operation.
- Each flight included 2 background preflight and postflight measurements for background and assessment of noise levels. The aircraft climbed to 500 m AGL (Above Ground Level) and maintained straight and level flight for one (1 minute or 5 km). A ‘background check’ was conducted at the beginning of each flight and repeated approximately every hour and after completing the last survey line of the flight.
- Each flight included 2 background measurements; preflight and postflight for TDEM compensation and collection of the reference waveform.
- A test line of a minimum of 5 km long, with a variety of conductive responses, was flown daily at survey height.

7.3. DAILY FIELD QUALITY CONTROL

7.3.1. GENERAL

- Check that all the files are on the server as expected.
- Download and unzip the files. Make sure they were complete and not corrupted.
- Check the header of the airborne raw data files to ensure the system was configured properly.
- Preprocess and then import the data into the Geosoft® software.
- Plot the flight path in Google Earth and Geosoft to verify that the data are complete and properly located and that the lines, as described in the flight logs, were flown.
- Check the flight path for crossing lines or lines that did not maintain proper separation.
- Plot the final flight path and look for problems, such as gaps and GPS busts.

7.3.2. ELECTROMAGNETIC DATA

- Visual check for shifts, excessive spiking, drift, etc.
- Correct/Compensate the EM data.

- Identify the backgrounds and measure/log the EM noise levels including original and compensated channels. Ensure they are within specification
- Filter the EM data and check for drift or offsets
- After splitting the GDB into lines, check again

7.3.3. MAGNETIC DATA AND MAGNETIC BASE STATION

- Check the start and end time of base station record and ensure that it covers the full survey data.
- Check the base station for cultural noise and diurnal activity. Ensure the diurnal is within specifications.
- Check the airborne magnetic data for gaps, dropouts, or excessive noise

7.3.4. ALTITUDE

- Visually check the altitude particularly at the start and ends of lines.
- Calculate the average helicopter altitude and ensure that it meets specifications.

7.4. QUALITY CONTROL IN THE OFFICE

Data verification was performed by experienced geophysicists in the processing centre or on-site using a work station that is capable of reading, analysing and duplicating the data on a daily basis. This system was available to MNDM (QA/QC geophysicist) to monitor data acquisition and verification.

The work flow diagram provided below (Figure 13) shows the tests and checks on data applied during the course of the survey and subsequent processing. The red lines represent feedback loops that will send data back to be reprocessed or even re-flown so as to correct for any deficiencies detected either in the field during QA/QC or at the Data Processing centre where senior staff review incoming data sets.

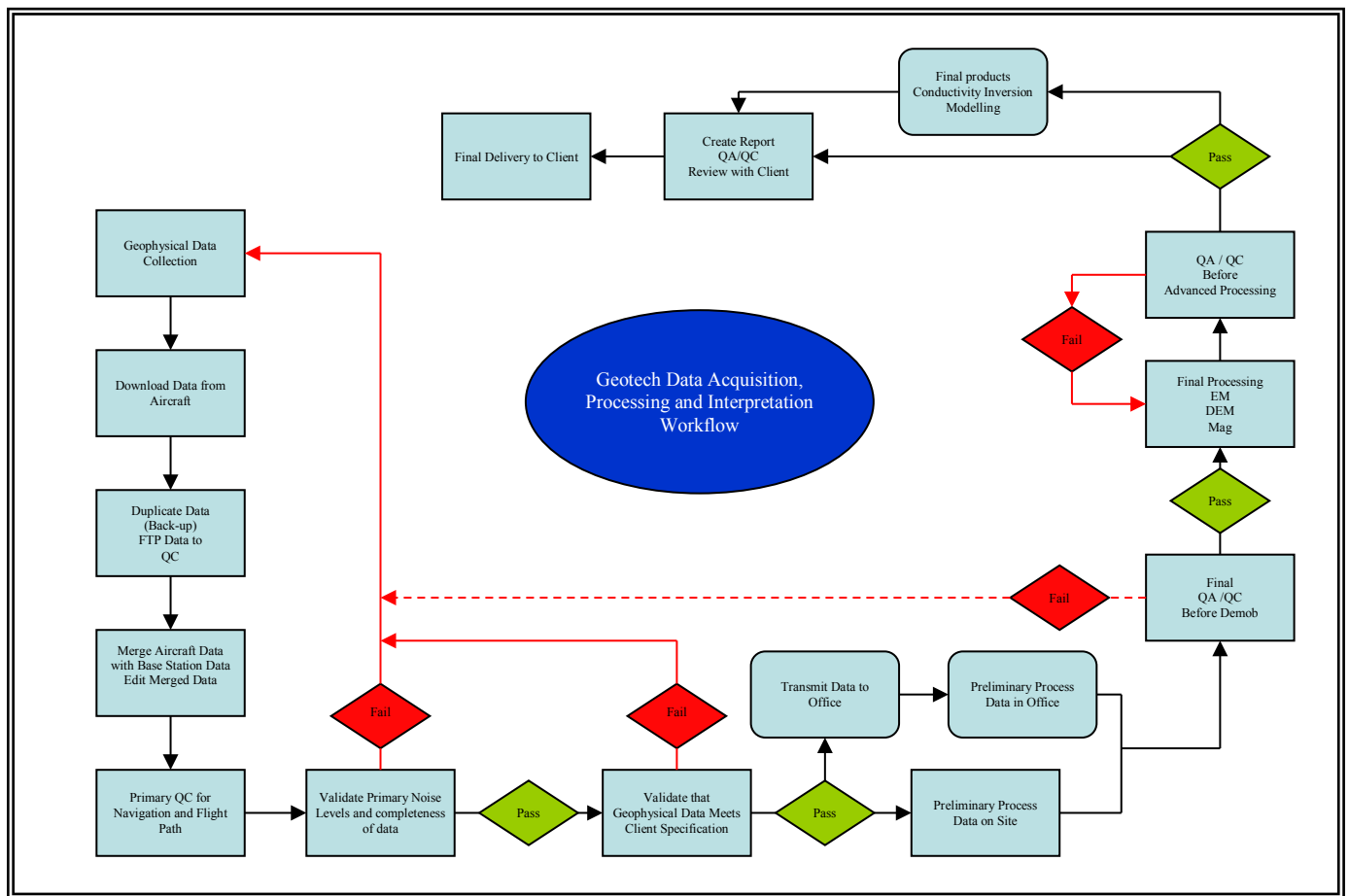


Figure 13. Data acquisition, data processing and interpretation workflow.

8. References

- Lewis, D. and Woolgar, S. 2011. Structural controls and alteration patterns of gold mineralization at Rowan Lake, northwest Ontario; *in* Summary of Field Work and Other Activities 2011, Ontario Geological Survey, Open File Report 6270, p.10-1 to 10-9.
- Keating, P.B. 1995. A simple technique to identify magnetic anomalies due to kimberlite pipes; *Exploration and Mining Geology*, v.4, no.2, p.121-125.
- Ontario Geological Survey 1999. Single master gravity and aeromagnetic data for Ontario; Ontario Geological Survey, Geophysical Data Set 1036.
- Ontario Geological Survey 2002. Ontario airborne geophysical surveys, magnetic and electromagnetic data, Vickers area; Ontario Geological Survey, Geophysical Data Set 1106rev.
- Ontario Geological Survey 2011. 1:250 000 scale bedrock geology of Ontario; Ontario Geological Survey, Miscellaneous Release—Data 126—Revision 1.
- Reford, S.W., Gupta, V.K., Paterson, N.R., Kwan, K.C.H. and Macleod, I.N. 1990. Ontario master aeromagnetic grid: A blueprint for detailed compilation of magnetic data on a regional scale; *in* Expanded Abstracts, Society of Exploration Geophysicists, 60th Annual International Meeting, San Francisco, v.1, p.617-619.
- Gupta, V., Paterson, N., Reford, S., Kwan, K., Hatch, D. and MacLeod, I. 1989. Single master aeromagnetic grid and magnetic colour maps for the province of Ontario; *in* Summary of Field Work and Other Activities 1989, Ontario Geological Survey, Miscellaneous Paper 146, p.244-250.
- McNeill, J.D. 1980. Applications of transient electromagnetic techniques, Technical Note 7, Geonics Ltd., Mississauga, Ontario.

Appendix A. GEOPHYSICAL DATA FILE LAYOUT

The files for the Nestor Falls Survey, Geophysical Data Set 1076, are archived on a single DVD. The content of the ASCII and Geosoft® binary file types are identical. They are provided in both forms to suit the user's available software. The survey data are divided as follows:

- Profile data
 - Profile database of electromagnetic and magnetic data (10 Hz sampling) in ASCII (XYZ) and Geosoft® Binary GDB formats
- Gridded data in ASCII (DXF) and Geosoft® Binary (GRD) formats:
 - total (residual) field magnetics
 - second vertical derivative of the total field magnetics
 - decay constant
 - apparent conductivity depth slices
 - digital elevation model
- EM anomaly database in ASCII (CSV) and Geosoft® Binary GDB formats
- Keating correlation coefficient database ASCII (CSV) and Geosoft® Binary GDB formats
- Vector files in DXF format:
 - flight path
 - EM anomalies
 - Keating correlation (kimberlite) anomalies
 - total field magnetic contours
 - decay constant contours
 - apparent conductivity contours
 - digital elevation model
- GEOTIFF images
 - colour total field magnetics with base map
 - colour shaded relief of second vertical derivative with base map
 - colour decay constant with base map
 - apparent conductivity depth slices with base map
- Waveform database in Geosoft® GDB format
- Conductivity Depth Imaging (CDI) data:
 - CDI database in Geosoft® Binary GDB format
 - Plotted CDI sections in portable document format, PDF
- Survey report in portable document format, PDF

Appendix B. PROFILE ARCHIVE DEFINITION

The profile data are provided in two formats, one binary and one ASCII.

ASCII XYZ and Geosoft® OASIS montaj™ binary database file (no compression) of electromagnetic, magnetic and ancillary data, sampled at 10 Hz

NFMAGEM.XYZ (ASCII)

NFMAGEM.GDB (Binary)

The contents of *.GDB/*.XYZ (both file types contain the same set of data channels) are summarized as follows:

Magnetic/Electromagnetic/ Ancillary Line Data

In NFMAGEM.XYZ, the electromagnetic channel data are provided in individual channels with numerical indices (e.g., em_z_final_off[14] to em_z_final_off[45]) along with magnetic and ancillary channels. In NFMAGEM.GDB, the electromagnetic channel data are provided in array channels with 32 elements.

Channel name	Units	Description
gps_x_raw	metres	raw GPS X
gps_y_raw	metres	raw GPS Y
gps_z_raw	metres	raw GPS Z
gps_x_final	decimal-degrees	differentially corrected GPS X (NAD83 datum)
gps_y_final	decimal-degrees	differentially corrected GPS Y (NAD83 datum)
gps_z_final	metres ASL	differentially corrected GPS Z (NAD83 datum)
x_nad83	metres	easting in UTM co-ordinates using NAD83 datum
y_nad83	metres	northing in UTM co-ordinates using NAD83 datum
lon_nad83	decimal-degrees	longitude using NAD83 datum
lat_nad83	decimal-degrees	latitude using NAD83 datum
radar_raw	metres above terrain	raw radar altimeter
radar_final	metres above terrain	corrected radar altimeter
dem	metres ASL	digital elevation model
fiducial		fiducial
flight		flight number
line_number		full flight line number(flight line and part numbers)
line		flight line number
time_utc	seconds	utc time
date	YYYYMMDD	local date
height_mag	metres above terrain	magnetometer height
mag_base_final	nanoteslas	corrected magnetic base station data
mag_raw	nanoteslas	raw magnetic field
mag_diurn	nanoteslas	diurnally-corrected magnetic field
mag_lev	nanoteslas	levelled magnetic field
igrf	nanoteslas	local IGRF field
mag_igrf	nanoteslas	IGRF-corrected magnetic field
mag_final	nanoteslas	diurnally and IGRF-corrected magnetic field
cvg	nanoteslas per metre	calculated magnetic vertical derivative from mag_final
mag_2vd	nanoteslas per square metre	calculated 2vd from mag_final
mag_gslevel	nanoteslas	GSC levelled magnetic field
cvg_gscl	nanoteslas per metre	calculated magnetic vertical derivative from mag_gslevel
mag_2vd_gscl	nanoteslas per square	calculated 2vd from gslevel

Report on Nestor Falls Area Airborne Geophysical Survey

Channel name	Units	Description
	metre	
height_em	metres above terrain	electromagnetic receiver height
em_z_raw_off	$(pV)/(A \cdot m^4)$	raw (stacked) dB/dt, Z-component, off-time channels 14 to 45
em_z_final_off	$(pV)/(A \cdot m^4)$	filtered and leveled dB/dt, Z-component, off-time channels 14 to 45
em_bz_raw_off	$(pV \cdot ms)/(A \cdot m^4)$	raw (stacked) B-field, Z-component, off-time channels 14 to 45
em_bz_final_off	$(pV \cdot ms)/(A \cdot m^4)$	filtered and leveled B-field, Z-component, off-time channels 14 to 45
power	microvolts	60 Hz power line monitor
tau_bz	microseconds	decay constant (tau) for B-field Z-component
tau_z	microseconds	decay constant (tau) for dB/dt Z-component
nchan_bz		latest time channels of TAU calculation, B-field Z
nchan_z		latest time channels of TAU calculation, dB/dt Z
appcond	Siemens per metre	apparent conductivity

Appendix C. EM ANOMALY ARCHIVE DEFINITION

The electromagnetic anomaly data are provided in two formats, one ASCII and one binary:

NFANOMALY.csv – ASCII comma-delimited Excel® format

NFANOMALY.gdb – Geosoft® OASIS montaj™ binary database file

Both file types contain the same set of data channels, summarized as follows:

Channel name	Units	Description
x_nad83	metres	easting in UTM co-ordinates using NAD83 datum
y_nad83	metres	northing in UTM co-ordinates using NAD83 datum
lon_nad83	decimal-degrees	longitude using NAD83 datum
lat_nad83	decimal-degrees	latitude using NAD83 datum
dem	metres asl	digital elevation model
fiducial		Fiducial
flight		flight number
line		flight line number
time_utc	seconds	utc time
date	YYYYMMDD	local date
em_z_final_off	$(pV)/(A*m^4)$	filtered and leveled dB/dt, Z-component, off-time channels 14 to 45
em_bz_final_off	$(pV*ms)/(A*m^4)$	filtered and leveled B-field, Z-component, off-time channels 14 to 45
tau_z	microseconds	decay constant (tau) for dB/dt Z-component
conductivity	Siemens per metre	apparent conductivity
height_em	metres above terrain	electromagnetic receiver height
anomaly_no		nth anomaly along the survey line
Anomaly_ID		Alpha identifier
anomaly_type_letter		anomaly classification, “thick” (K) or “thin” (N) anomaly
anomaly_type_no		anomaly classification (i.e. anomaly grade), 1 to 6 from the weakest to the strongest
Conductance_dbdt	Siemens	apparent conductance, calculated from dB/dt data
Conductance_bfield	Siemens	apparent conductance, calculated from B-field data
depth_to_conductor	metres	Depth to conductor
heading	degrees	direction of flight
survey_number		Government survey number
Nchan_z		Number of off-time channels deflected

Appendix D. KEATING CORRELATION ARCHIVE DEFINITION

The Keating kimberlite pipe correlation coefficient data are provided in 2 formats, one ASCII and one binary:

MCKC.csv – ASCII comma-delimited format

MCKC.gdb – Geosoft® OASIS montaj™ binary database file

Both file types contain the same set of data channels, summarized as follows:

Channel name	Units	Description
x_nad83	metres	easting in UTM co-ordinates using NAD83 datum
y_nad83	metres	northing in UTM co-ordinates using NAD83 datum
lon_nad83	decimal-degrees	longitude using NAD83 datum
lat_nad83	decimal-degrees	latitude using NAD83 datum
corr_coeff	percent	correction coefficient
pos_coeff	percent	positive correction coefficient
neg_coeff	percent	negative correction coefficient
norm_error	percent	standard error normalized to amplitude
amplitude	nanoteslas	peak-to-peak anomaly amplitude within window

Appendix E. GRID ARCHIVE DEFINITION

The gridded data are provided in 2 formats, one ASCII and one binary:

*.gxf - Geosoft® ASCII Grid eXchange Format (no compression)

*.grd - Geosoft® OASIS montaj™ binary grid file (no compression)

All grids are NAD83 UTM Zone 15 North, with a grid cell size of 40 m x 40 m.

Grids in Geosoft GRD and GXF format, as follows:

The grids are summarized as follows:

- NFMAG83: Total Magnetic Intensity (nT)
- NF2VD83: Second Calculated Vertical Derivative of TMI (nT/m²)
- NFDEM83: Digital Elevation Model (metres)
- NFDCZ83: TDEM Decay Constant Z Component
- NFCON83: TDEM Apparent Conductivity depth slice 100m below surface (mS/m)
- NFCON83_ *dd*: TDEM Apparent Conductivity depth slices (mS/m)

Where *dd* represents the level of depth in metres (0, -100, -200, -300)

A Geosoft .GRD file has a .GI metadata file associated with it, containing grid projection information.

Appendix F. GEOTIFF AND VECTOR ARCHIVE DEFINITION

GeoTIFF Images

Geographically referenced colour images, incorporating a planimetric base, are provided in GeoTIFF format for use in GIS applications:

- NFMAG83.TIF – Colour residual, GSC levelled, magnetic field grid plotted on a planimetric base
- NF2VD83.TIF – Shaded colour image of the second vertical derivative of the residual magnetic field on a planimetric base
- NFDCZ83.TIF – Colour decay constant on a planimetric base
- NFCON83.TIF – Colour apparent conductivity on a planimetric base 100 m below surface
- NFCON83_ *dd*.TIFF - TDEM apparent conductivity depth slices
Where *dd* represents the level of depth in metres (0, -100, -200, -300)

Vector Archives

Vector line work from the map is provided in DXF (v12) ASCII format using the following naming convention:

- NFPATH83.DXF – flight path of the survey area
- NFKC83.DXF – Keating correlation targets
- NFMAG83.DXF – contours of the GSC levelled, residual magnetic field in nT
- NFDCZ83.DXF – contours of the Z coil decay constant in μsec
- NFCON83.DXF – contours of the apparent conductivity 100 m below surface in (mS/m)
- NFANOMALY83.DXF – electromagnetic anomaly symbols

The layers within the DXF files correspond to the various object types found therein and have intuitive names.

Appendix G. WAVEFORM AND CONDUCTIVITY DEPTH IMAGE ARCHIVE DEFINITION

The databases of the transmitter reference waveform and the Conductivity Depth Image (CDI) are provided in binary format:

Transmitter Reference Waveform

NFMAGEM_Reference Waveform.gdb – Geosoft® OASIS montaj™ binary database file

Conductivity Depth Image

NFMAGEM_Reference Waveform.gdb – Geosoft® OASIS montaj™ binary database file

Descriptions of the data channels are provided below

Geosoft database for the VTEM waveform

Channel name	Description
Time:	Sampling rate interval, 5.2083 milliseconds
Tx_Current:	Output current of the transmitter (amps)

Geosoft database for conductivity depth image (CDI) data format

Channel name	Units	Description
xg	metres	easting in UTM co-ordinates using NAD83 datum
yg	metres	northing in UTM co-ordinates using NAD83 datum
dist	metres	distance from the beginning of the line
depth	metres	array channel, depth from the surface
z	metres	array channel, depth from sea level
appres	ohm.m	array channel, apparent resistivity
appcond	Siemens per metre	array channel, apparent conductivity
tr	metres	electromagnetic receiver height from sea level
topo	metres	digital elevation model
height_em	metres	electromagnetic receiver height
em_z_final_off	pV/(A*m ⁴)	array channel, filtered and leveled dB/dt, Z-component, off-time channels 14 to 45
mag_gslevel	nanoteslas	GSC levelled magnetic field
cvg_gscl	nanoteslas per metre	calculated magnetic vertical derivative from mag_gslevel
doi	metres	Depth of Investigation: a measure of VTEM depth effectiveness
power		60Hz power line monitor

In addition PDF files of plotted CDI sections (one per flight line) are presented in the following files:

NFMAGEM_CDI_Sections_All_Lines(mutli zon files) – CDI sections with individual colour schemes

NFMAGEM_CDI_Sections_All_Lines(single zon files) – CDI sections with common colour scheme

Appendix H. SURVEY BLOCK CO-ORDINATES

(WGS 84, UTM Zone 15 North)

X	Y	Continued	
		X	Y
421900	5483650		
421900	5447600	458400	5460200
426400	5447550	447100	5460200
435000	5440950	440900	5473600
444000	5435500	440900	5476100
444000	5427700	444700	5481350
450600	5425300	444700	5483650
450600	5427600	421900	5483650
453550	5427600	426500	5450100
453550	5429600	426500	5453600
457150	5429600	430700	5459550
457150	5431600	433100	5459550
463000	5431600	434950	5458250
463000	5433600	437300	5461600
467050	5433600	438800	5461600
467050	5434500	448000	5454750
481000	5434500	448000	5451600
481000	5446700	445200	5451600
472300	5446700	441250	5446000
472300	5471000	438950	5447600
467050	5471000	436150	5447600
467050	5469650	436150	5450100
458400	5469650	426500	5450100

Appendix I. GENERAL MODELING RESULTS OF THE VTEM SYSTEM

Introduction

The VTEM system is based on a concentric or central loop design, whereby, the receiver is positioned at the centre of a transmitter loop that produces a primary field. The wave form is a bipolar, modified square wave with a turn-on and turn-off at each end.

During turn-on and turn-off, a time varying field is produced (dB/dt) and an electromotive force (emf) is created as a finite impulse response. A current ring around the transmitter loop moves outward and downward as time progresses. When conductive rocks and mineralization are encountered, a secondary field is created by mutual induction and measured by the receiver at the centre of the transmitter loop.

Efficient modeling of the results can be carried out on regularly shaped geometries, thus yielding close approximations to the parameters of the measured targets. The following is a description of a series of common models made for the purpose of promoting a general understanding of the measured results.

A set of models has been produced for the Geotech VTEM[®]Plus system dB/dt Z and X components (see models I-1 to I-17). The Maxwell[™] modeling program (EMIT Technology Pty. Ltd. Midland, WA, AU) used to generate the following responses assumes a resistive half-space. The reader is encouraged to review these models, so as to get a general understanding of the responses as they apply to survey results. While these models do not begin to cover all possibilities, they give a general perspective on the simple and most commonly encountered anomalies.

As the plate dips and departs from the vertical position, the peaks become asymmetrical.

As the dip increases, the aspect ratio (Min/Max) decreases and this aspect ratio can be used as an empirical guide to dip angles from near 90° to about 30°. The method is not sensitive enough where dips are less than about 30°.

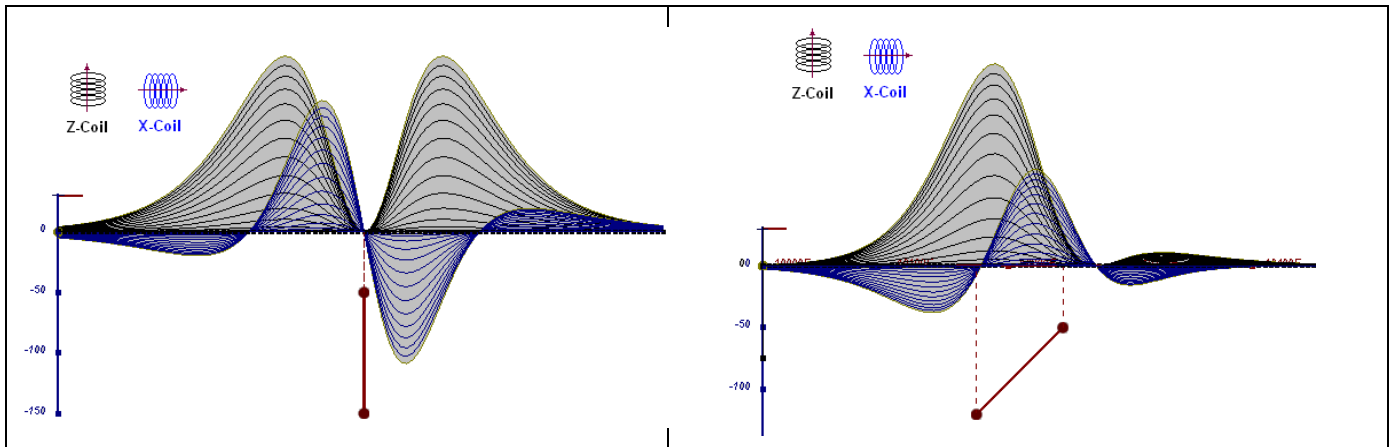


Figure I-1. vertical thin plate

Figure I-2. inclined thin plate

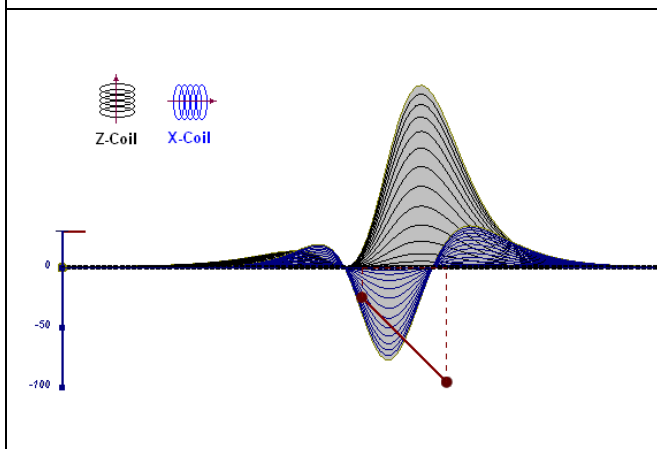


Figure I-3. inclined thin plate

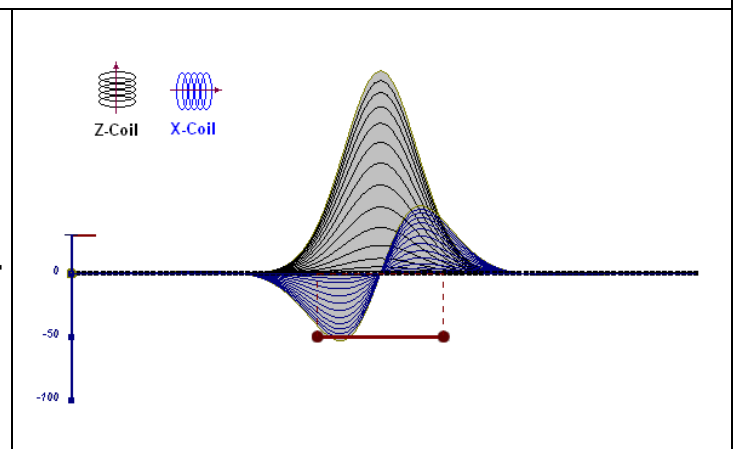


Figure I-4. horizontal thin plate

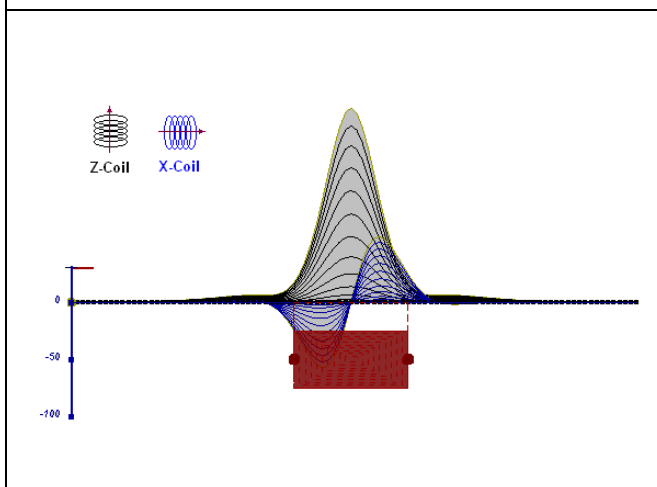


Figure I-5. horizontal thick plate (linear scale of the response)

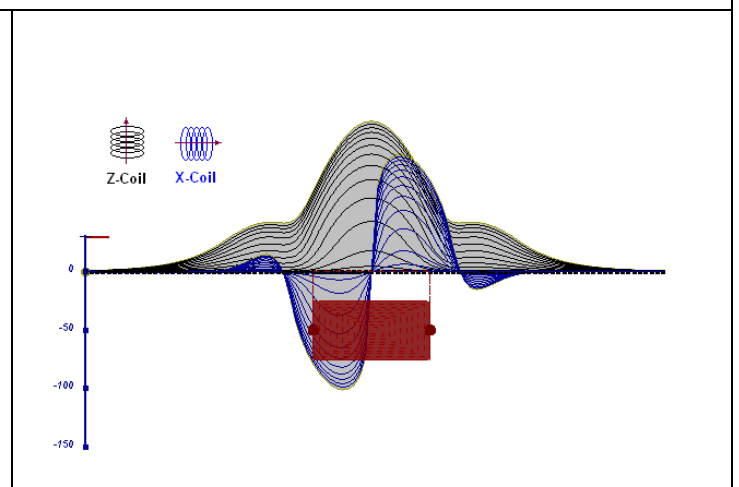


Figure I-6. horizontal thick plate (log scale of the response)

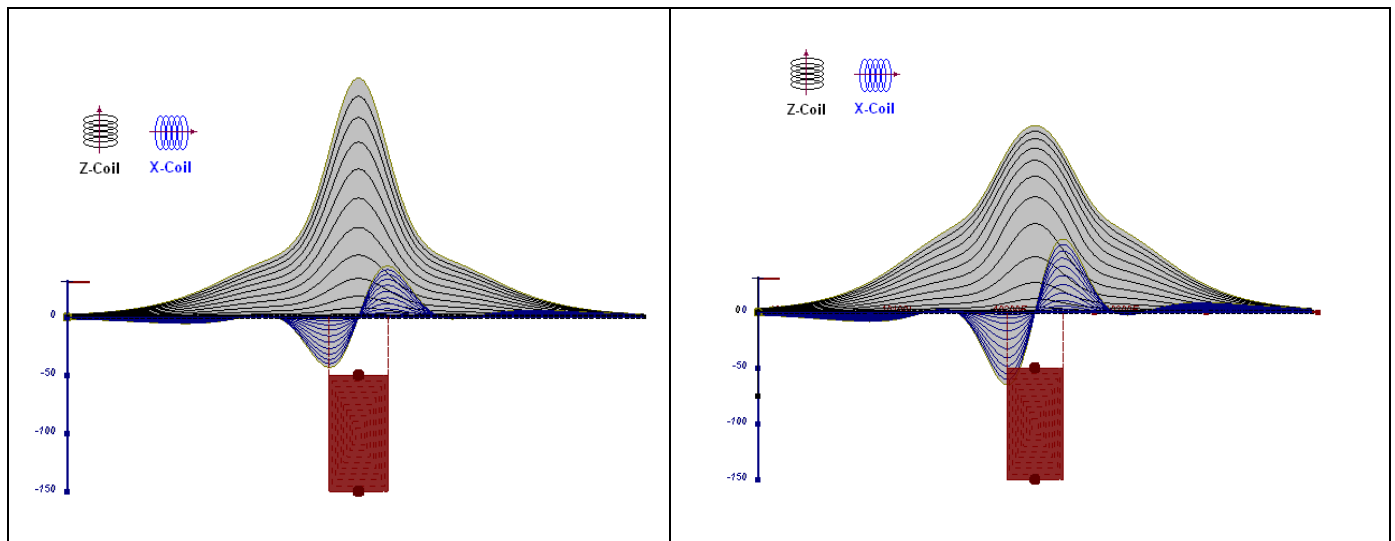


Figure I-7. vertical thick plate (linear scale of the response). 50 m depth

Figure I-8. vertical thick plate (log scale of the response). 50 m depth

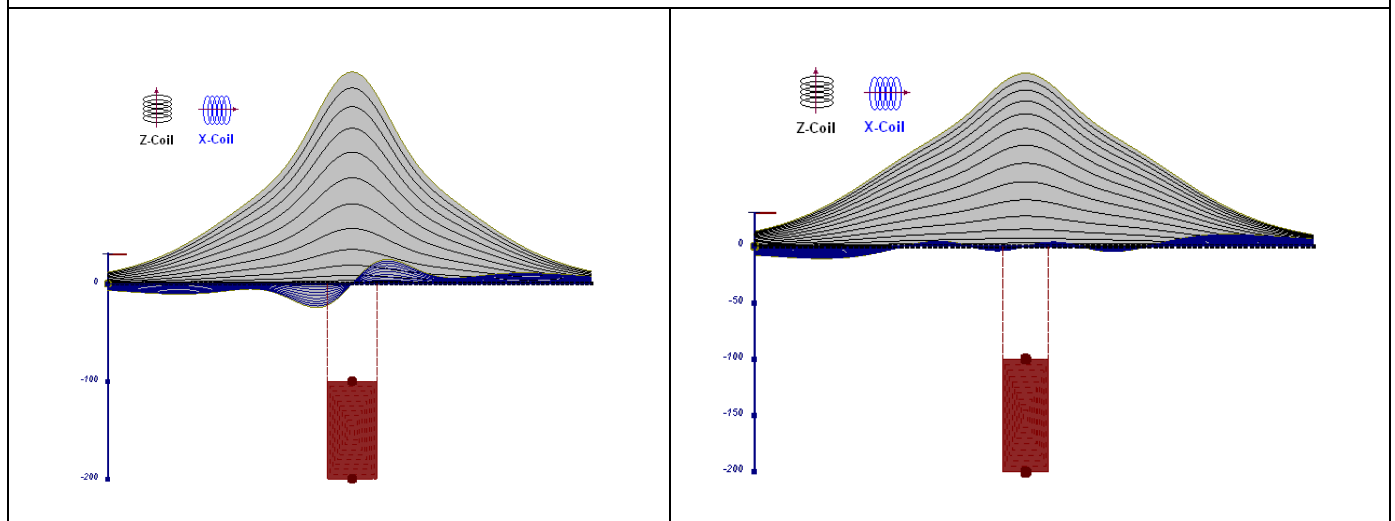


Figure I-9. vertical thick plate (linear scale of the response). 100 m depth

Figure I-10. vertical thick plate (linear scale of the response). Depth/hor.thickness=2.5

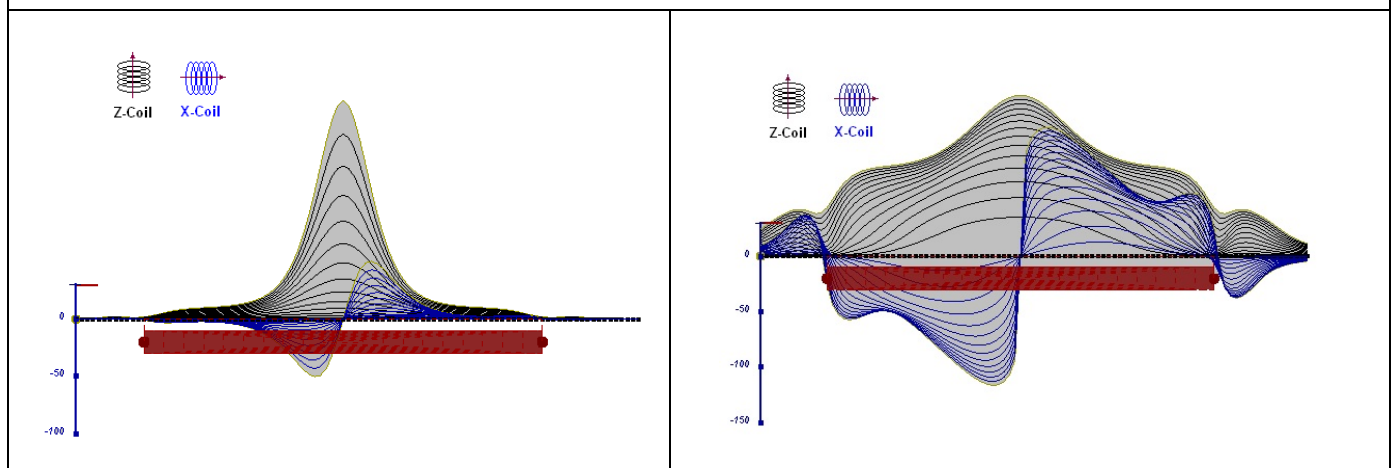


Figure I-11. horizontal thick plate (linear scale of the response)

Figure I-12. horizontal thick plate (log scale of the response)

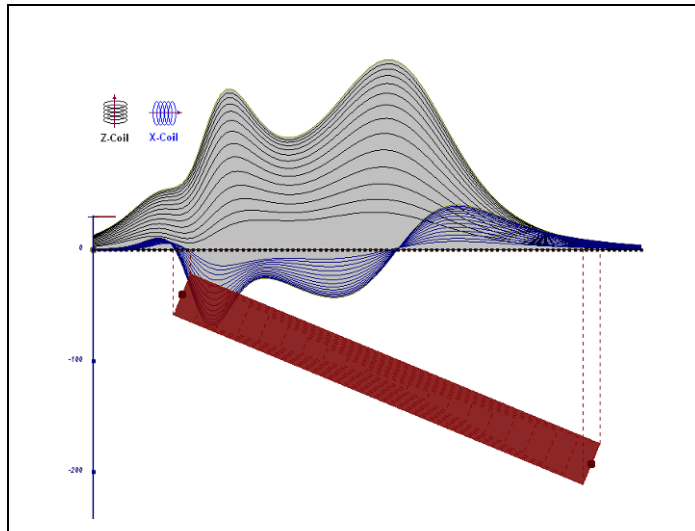


Figure I-13. inclined long thick plate

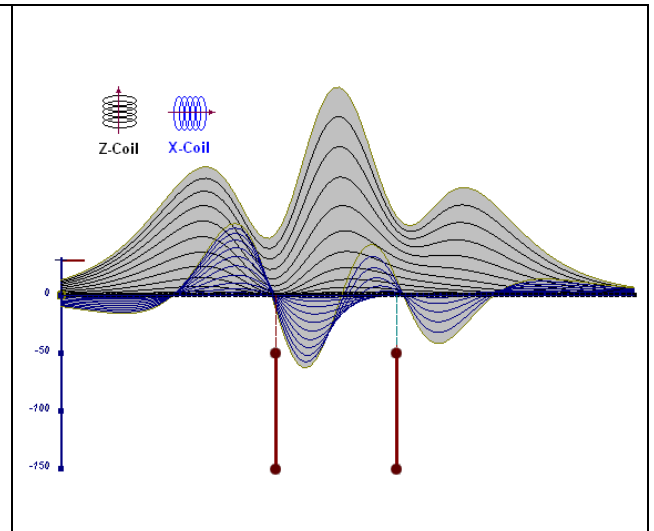


Figure I-14. two vertical thin plates

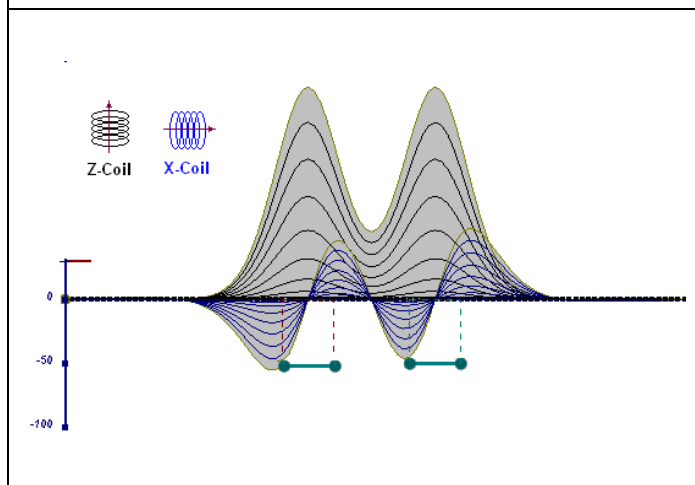


Figure I-15. two horizontal thin plates

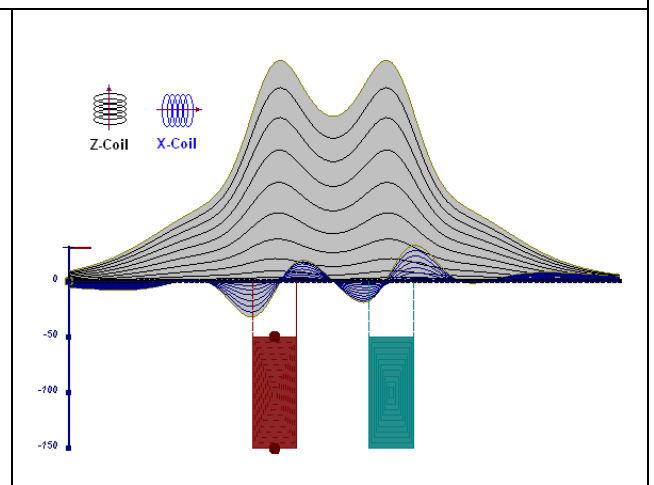


Figure I-16. two vertical thick plates

The same type of target but with different thickness, for example, creates different form of the response:

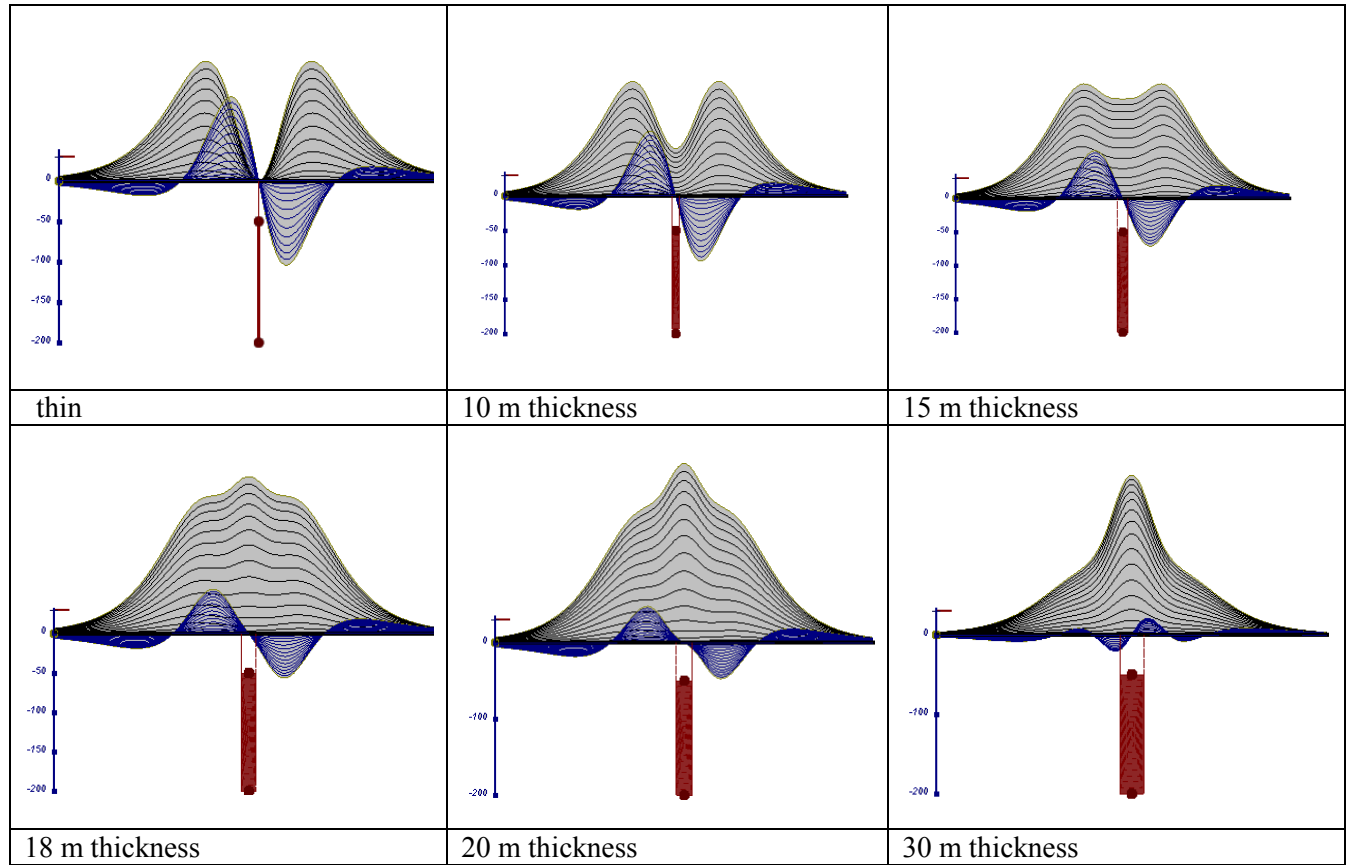


Figure I-17. Conductive vertical plate, depth 50 m, strike length 200 m, depth extend 150 m.

Alexander Prikhodko, PhD, *P. Geo.*

Geotech Ltd.

September 2010

Appendix J. EM TIME CONSTANT (TAU) ANALYSIS

Estimation of time constant parameter⁴ in transient electromagnetic method is one of the steps toward the extraction of the information about conductances beneath the surface from TEM measurements.

The most reliable method to discriminate or rank conductors from overburden, background or one and other is by calculating the EM field decay time constant (TAU parameter), which directly depends on conductance despite their depth and accordingly amplitude of the response.

Theory

As established in electromagnetic theory, the magnitude of the electro-motive force (emf) induced is proportional to the time rate of change of primary magnetic field at the conductor. This emf causes eddy currents to flow in the conductor with a characteristic transient decay, whose Time Constant (Tau) is a function of the conductance of the survey target or conductivity and geometry (including dimensions) of the target. The decaying currents generate a proportional secondary magnetic field, the time rate of change of which is measured by the receiver coil as induced voltage during the Off time.

The receiver coil output voltage (e_0) is proportional to the time rate of change of the secondary magnetic field and has the form,

$$e_0 \propto (1 / \tau) e^{-(t/\tau)}$$

Where,

$\tau = L/R$ is the characteristic time constant of the target (TAU)

R = resistance

L = inductance

From the expression, conductive targets that have small value of resistance and hence large value of τ yield signals with small initial amplitude that decays relatively slowly with progress of time. Conversely, signals from poorly conducting targets that have large resistance value and small τ , have high initial amplitude but decay rapidly with time¹ (Figure J-1).

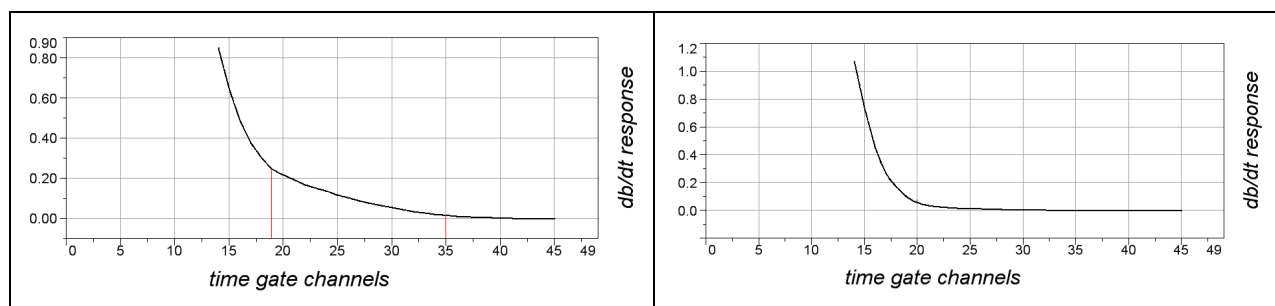


Figure J-1. Left – presence of good conductor, right – poor conductor.

⁴ McNeill, JD, 1980, "Applications of Transient Electromagnetic Techniques", Technical Note TN-7 pg 5, Geonics Limited, Mississauga, Ontario.

EM Time Constant (Tau) Calculation

The EM Time-Constant (TAU) is a general measure of the speed of decay of the electromagnetic response and indicates the presence of eddy currents in conductive sources as well as reflecting the “conductance quality” of a source. Although TAU can be calculated using either the measured dB/dt decay or the calculated B-field decay, dB/dt is commonly preferred due to better stability (S/N) relating to signal noise. Generally, TAU calculated on base of early time response reflects both near surface overburden and poor conductors whereas, in the late ranges of time, deep and more conductive sources, respectively. For example early time TAU distribution in an area that indicates conductive overburden is shown in Figure J-2. In Figure J-3, the full time range is displayed, showing the expression of a deep, highly-conductive target in the left side of the image.

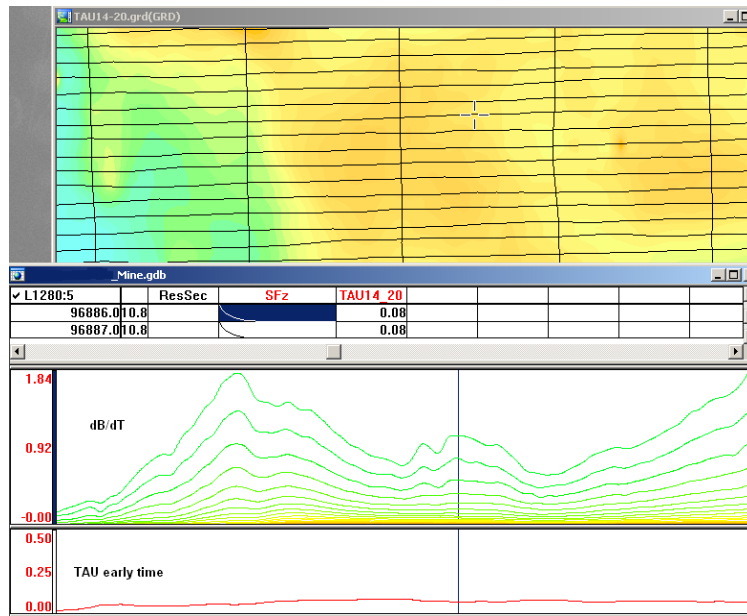


Figure J-2. Map of early time TAU. Area with overburden conductive layer and local sources.

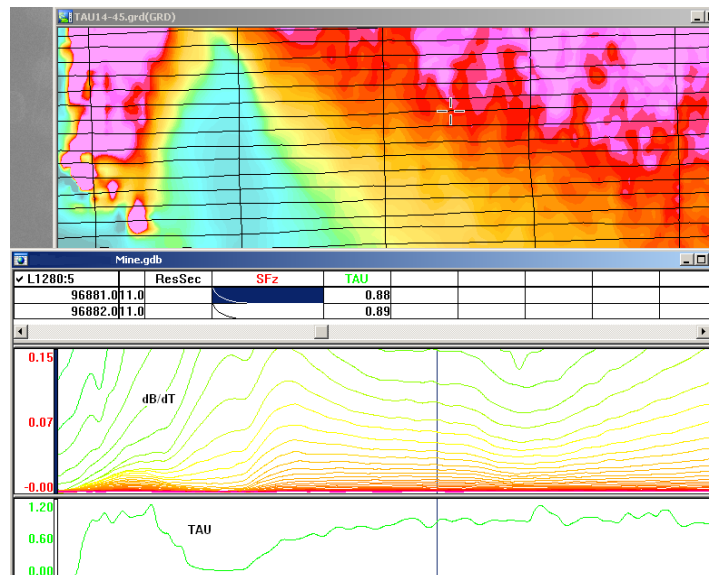


Figure J-3. Map of full time range TAU with EM anomaly due to deep highly conductive target.

There are many advantages of TAU maps:

- TAU depends only on one parameter (conductance) in contrast to response magnitude;
- TAU is integral parameter, which covers time range and all conductive zones and targets are displayed independently of their depth and conductivity on a single map.
- Very good differential resolution in complex conductive places with many sources with different conductivity.
- Signs of the presence of good conductive targets are amplified and emphasized independently of their depth and level of response accordingly.

In the example shown in figures J-4 and J-5, 3 local targets are defined, each of them with a different depth of burial, as indicated on the resistivity depth image (RDI). All are very good conductors but the deeper target (number 2) has a relatively weak dB/dt signal yet also features the strongest total TAU (Figure J-4). This example highlights the benefit of TAU analysis in terms of an additional target discrimination tool.

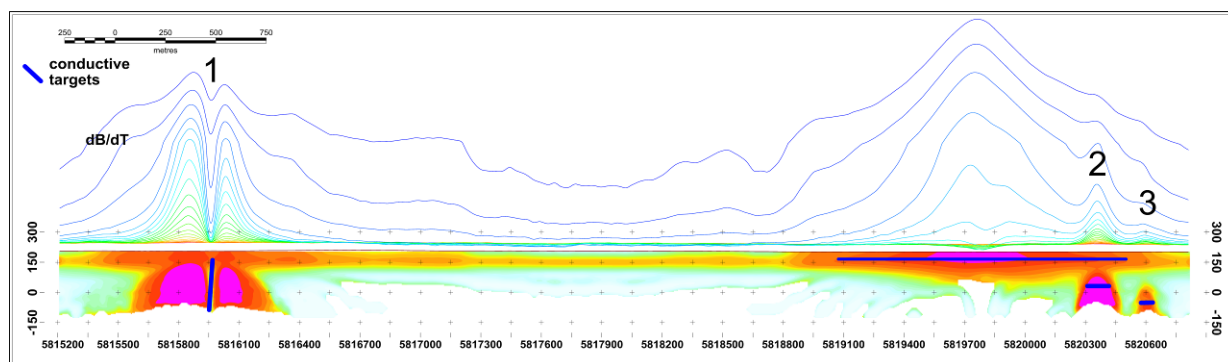


Figure J-4. dB/dt profile and RDI with different depths of targets.

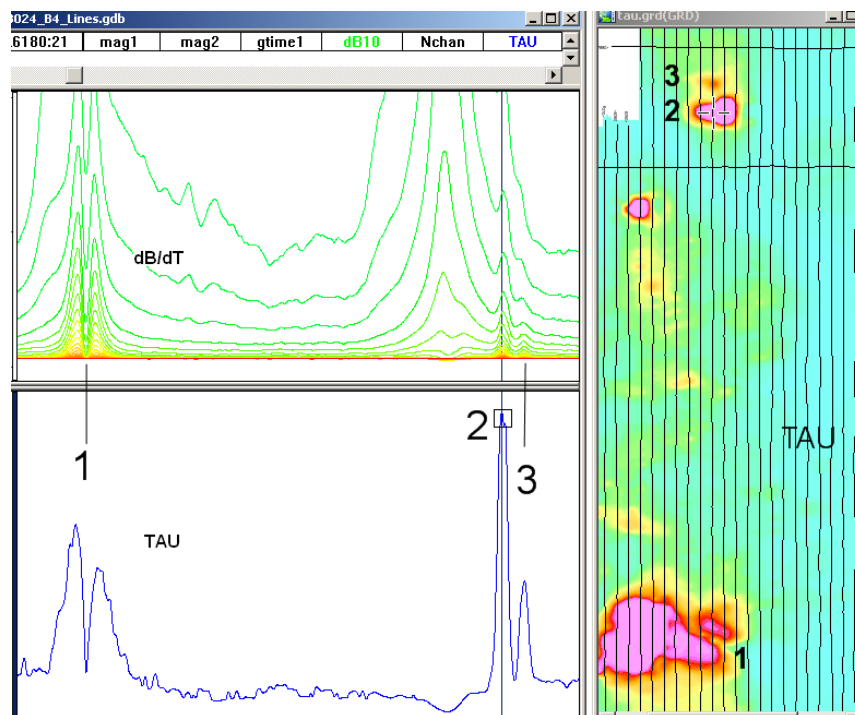


Figure J-5. Map of total TAU and dB/dt profile.

The EM Time Constants for dB/dt and B-field were calculated using the “sliding Tau” in-house program developed at Geotech⁵. The principle of the calculation is based on using of time window (4 time channels) which is sliding along the curve decay and looking for latest time channels which have a response above the level of noise and decay. The EM decays are obtained from all available decay channels, starting at the latest channel. Time constants are taken from a least square fit of a straight-line (log/linear space) over the last 4 gates above a preset signal threshold level (Figure J-6). Threshold settings are pointed in the “label” property of TAU database channels. The sliding Tau method determines that, as the amplitudes increase, the time-constant is taken at progressively later times in the EM decay. Conversely, as the amplitudes decrease, Tau is taken at progressively earlier times in the decay. If the maximum signal amplitude falls below the threshold, or becomes negative for any of the 4 time gates, then Tau is not calculated and is assigned a value of “dummy” by default.

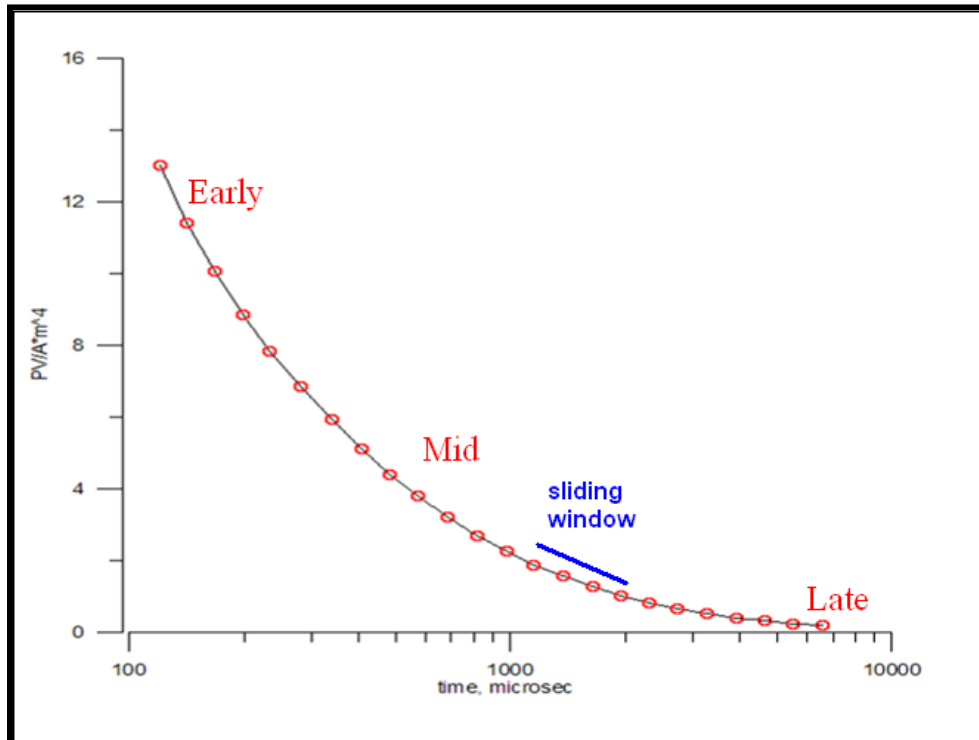


Figure J-6. Typical dB/dt decays of VTEM data

Alexander Prikhodko, PhD, *P. Geo.*

Geotech Ltd.

September 2010

⁵ Geotech Ltd. internal report by A.Prikhodko

Appendix K. TEM RESISTIVITY DEPTH IMAGING (RDI)

Resistivity depth imaging (RDI) is technique used to rapidly convert EM profile decay data into an equivalent resistivity versus depth cross-section, by deconvolution of the measured TEM data. The used RDI algorithm of Resistivity-Depth transformation is based on scheme of the apparent resistivity transform of Maxwell A.Meju (1998)⁶ and TEM response from conductive half-space. The program was developed by Alexander Prikhodko and depth calibrated based on forward plate modeling for VTEM system configuration (Figures K-1 to 11).

RDI's provide reasonable indications of conductor relative depth and vertical extent, as well as accurate 1D layered-earth apparent conductivity/resistivity structure across VTEM flight lines.

Approximate depth of investigation of a TEM system, image of secondary field distribution in half space, effective resistivity, initial geometry and position of conductive targets is the information obtained on base of the RDI's.

Maxwell forward modeling with RDI sections from the synthetic responses (VTEM system)

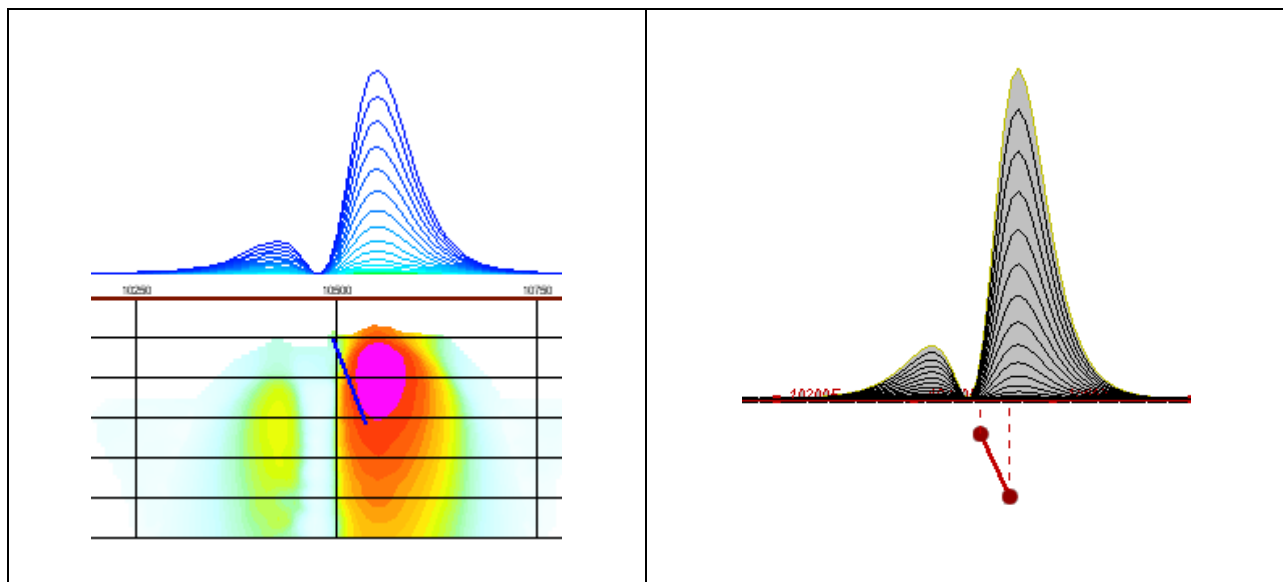


Figure K-1. Maxwell plate model and RDI from the calculated response for conductive “thin” plate (depth 50 m, dip 65 degree, depth extend 100 m).

⁶ Meju, M.A. 1998. Short Note: A simple method of transient electromagnetic data analysis, *Geophysics*, **63**, 405–410.

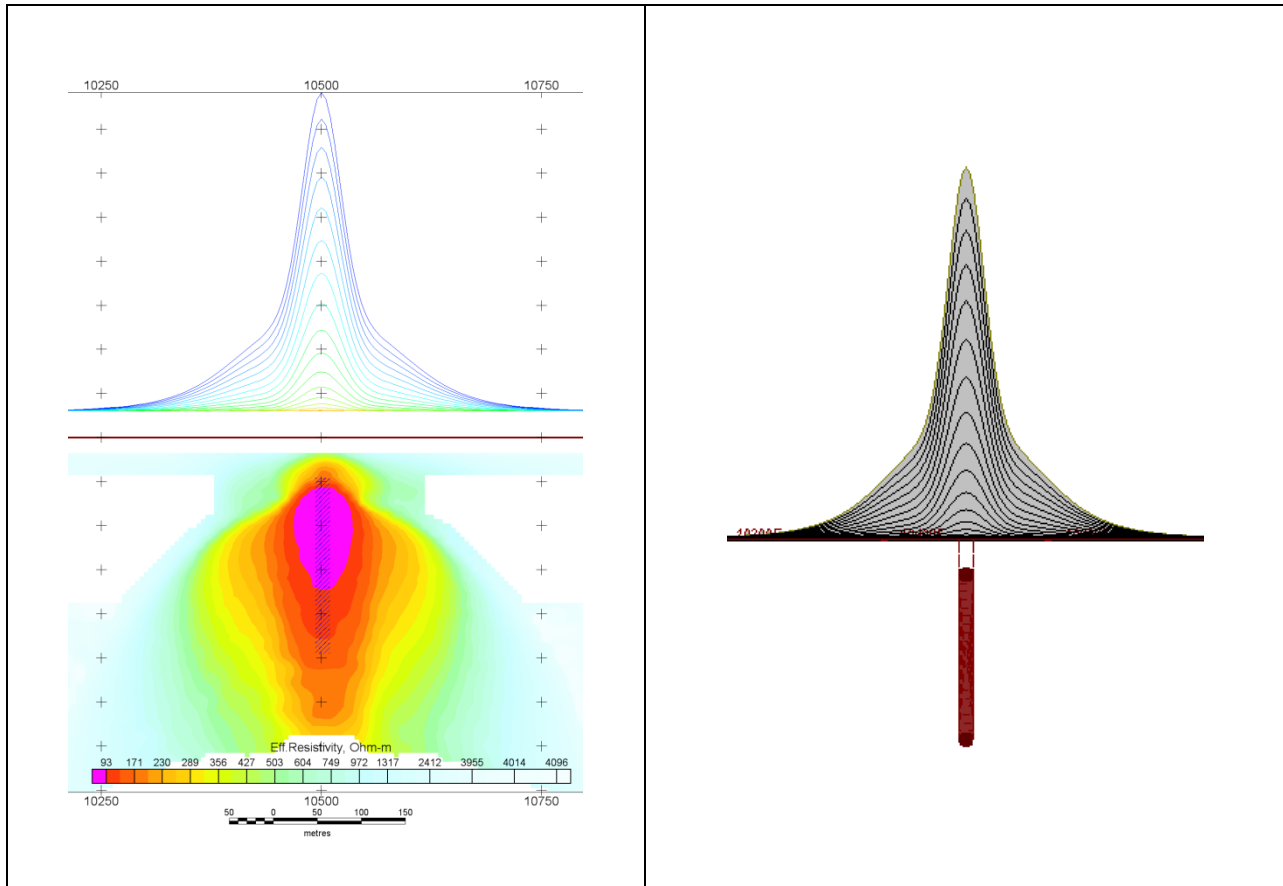


Figure K-2. Maxwell plate model and RDI from the calculated response for “thick” plate 18 m thickness, depth 50 m, depth extend 200 m).

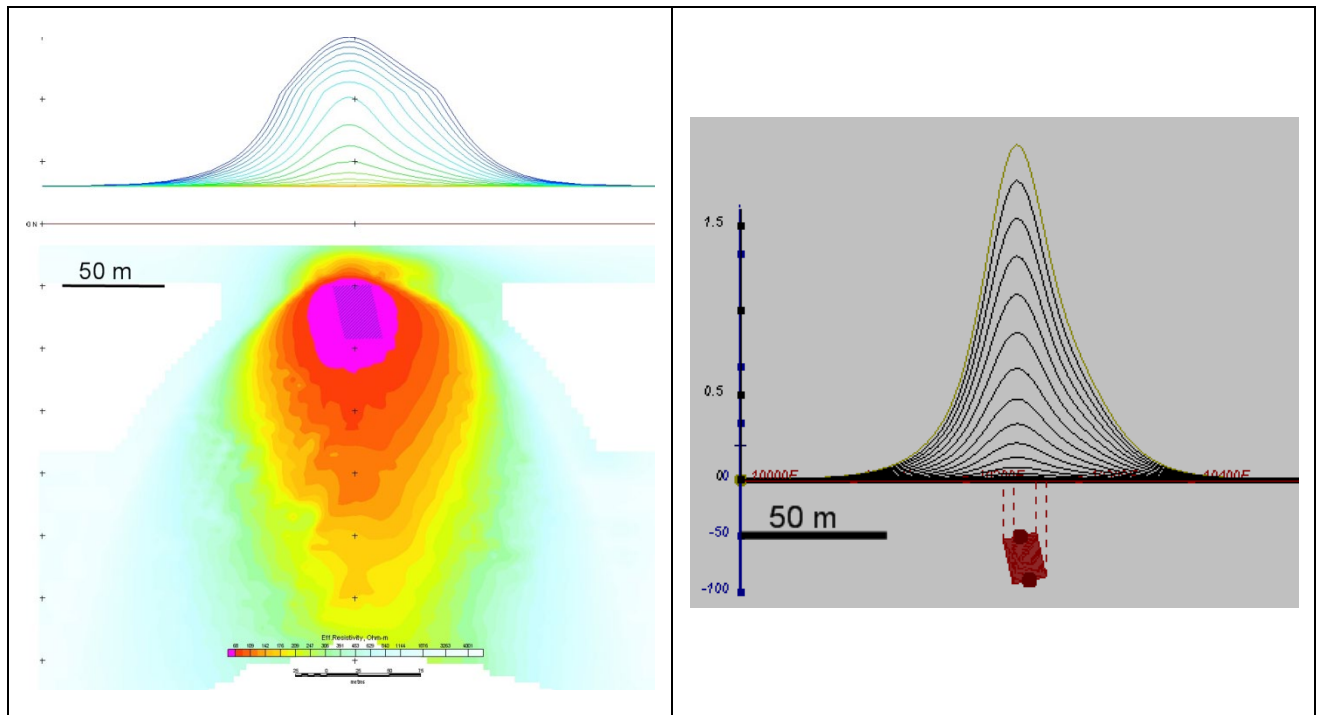


Figure K-3. Maxwell plate model and RDI from the calculated response for bulk (“thick”) 100 m length, 40 m depth extend, 30 m thickness.

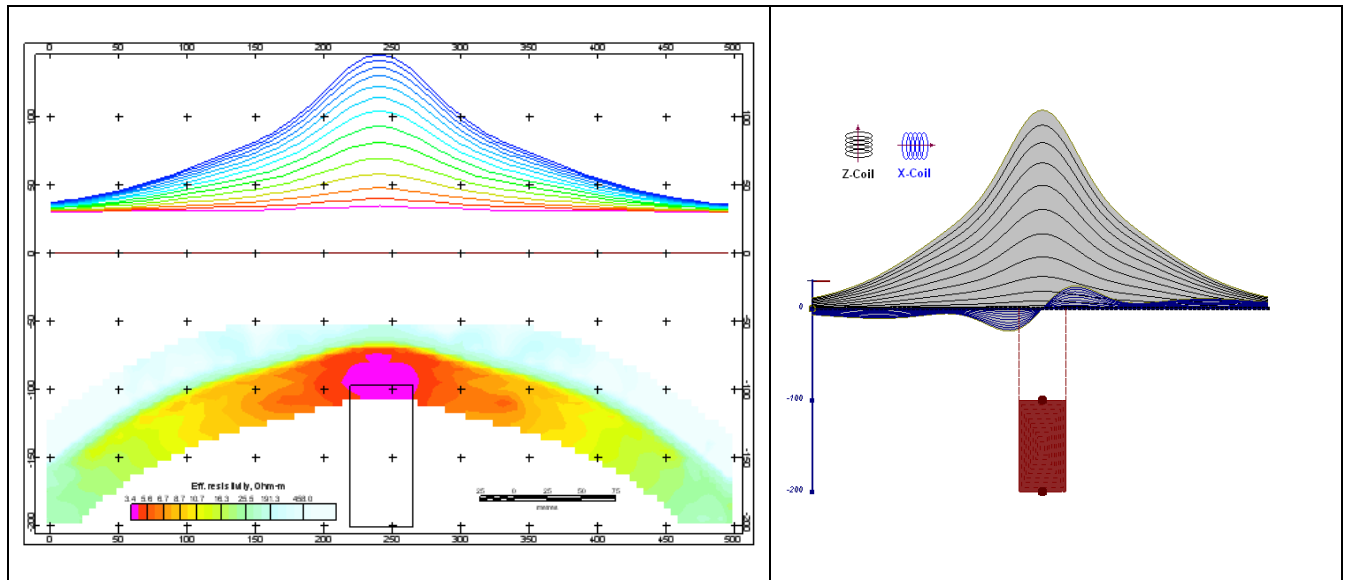


Figure K-4. Maxwell plate model and RDI from the calculated response for “thick” vertical target (depth 100 m, depth extend 100 m). 19-44 channels.

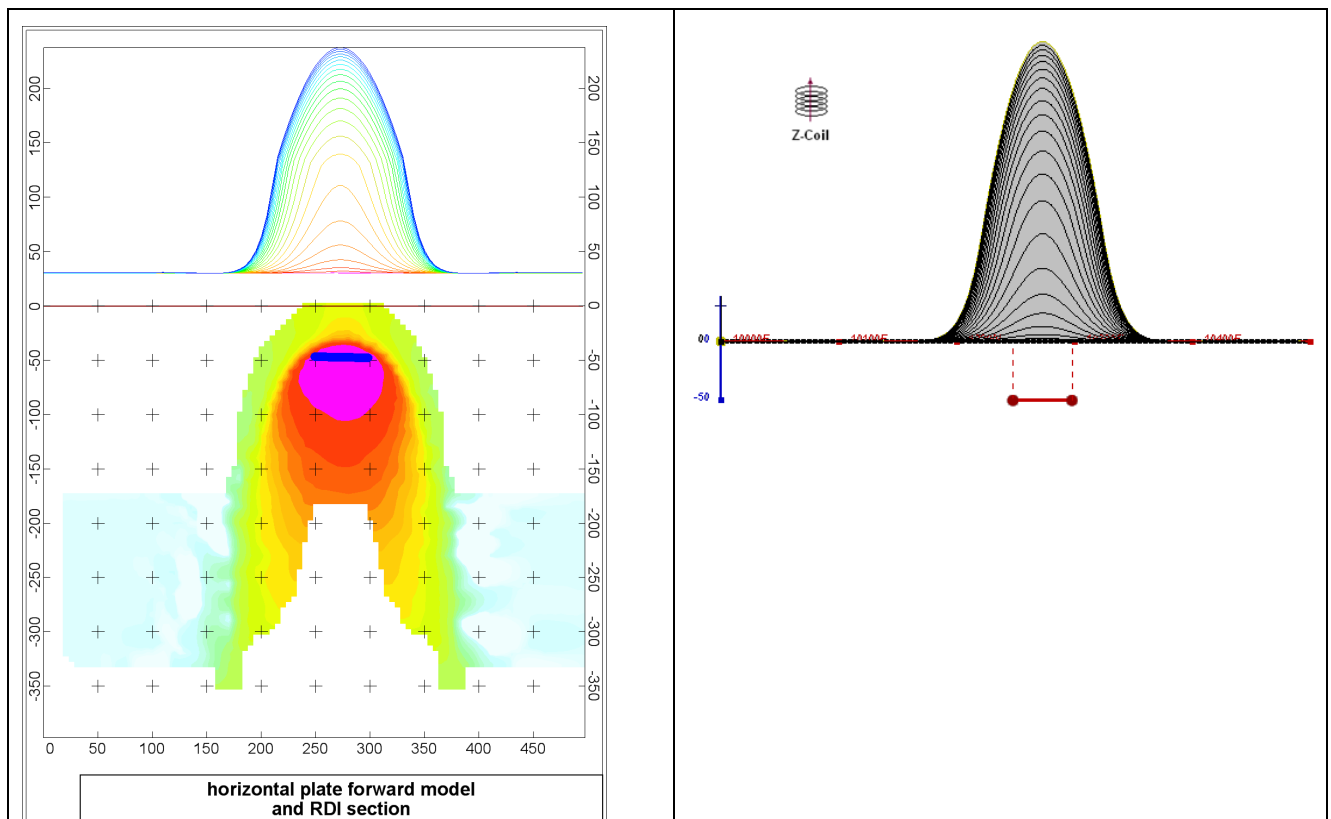


Figure K-5. Maxwell plate model and RDI from the calculated response for horizontal thin plate (depth 50 m, dim 50x100 m). 15-44 channels.

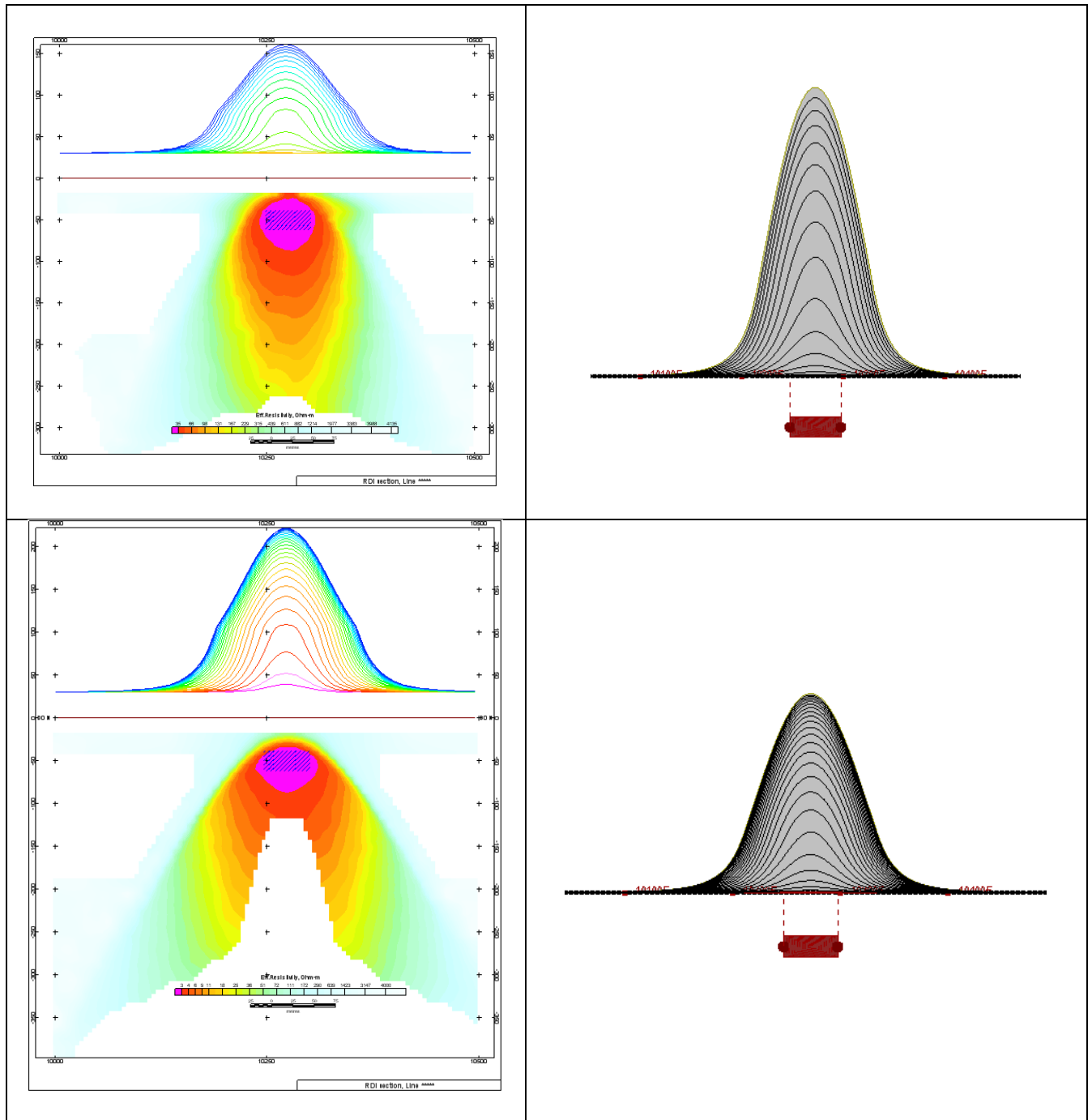


Figure K-6. Maxwell plate model and RDI from the calculated response for horizontal thick (20m) plate – less conductive (on the top), more conductive (below)

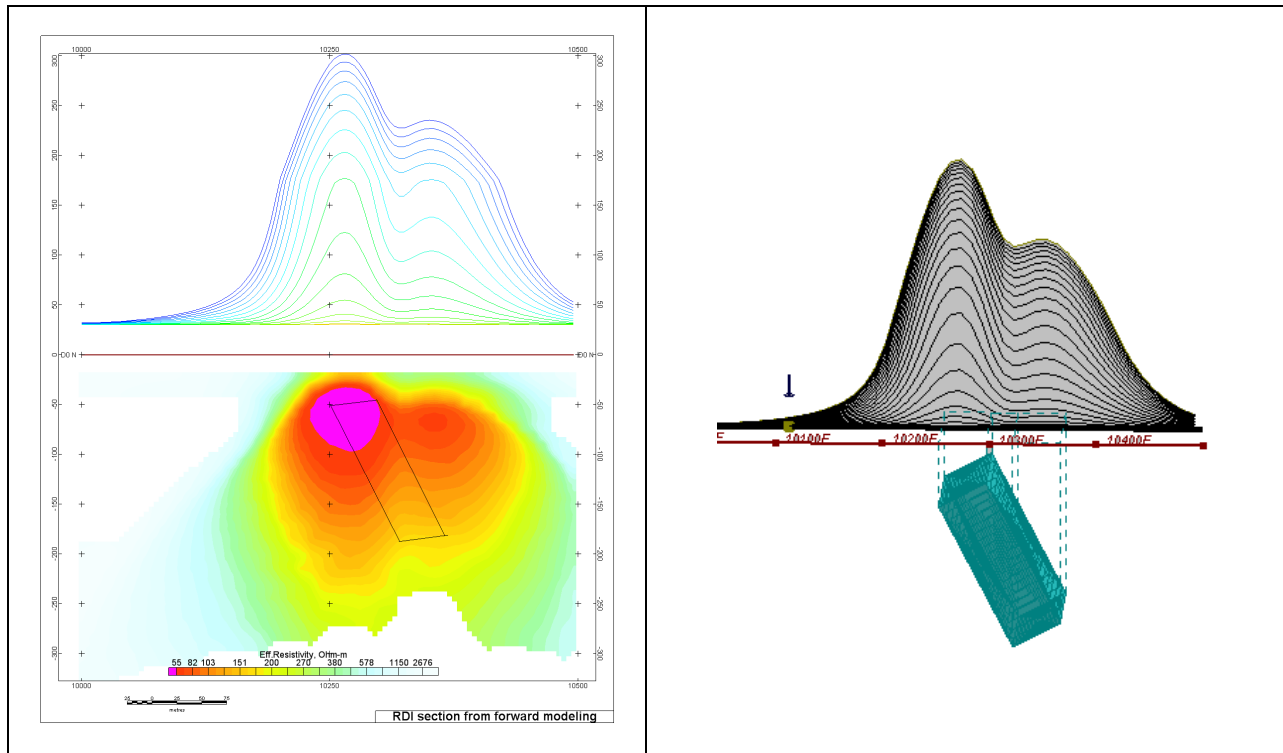


Figure K-7. Maxwell plate model and RDI from the calculated response for inclined thick (50m) plate. Depth extends 150 m, depth to the target 50 m.

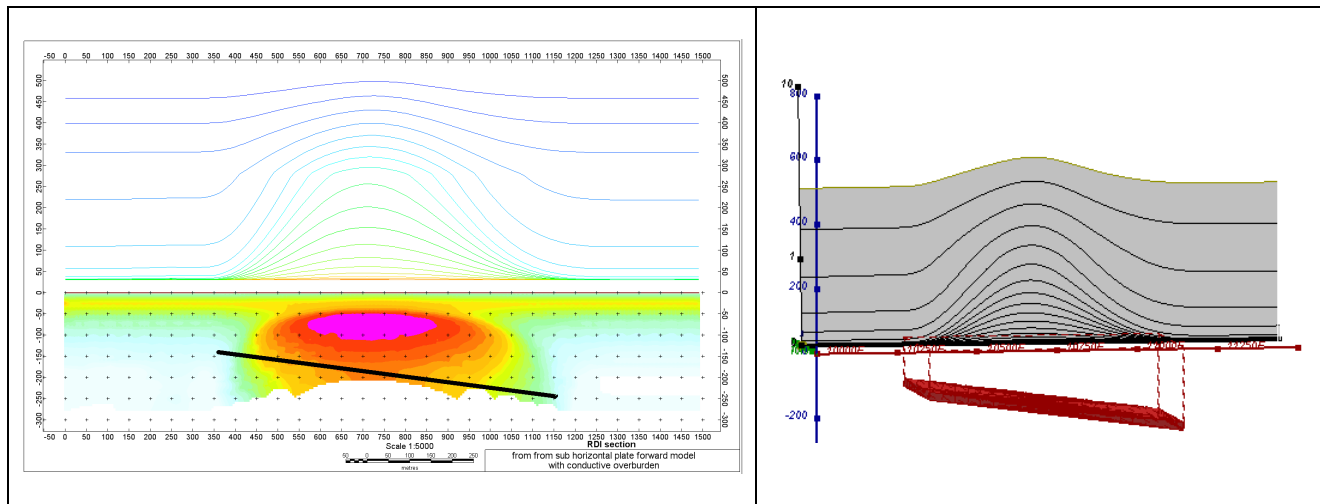


Figure K-8. Maxwell plate model and RDI from the calculated response for the long, wide and deep sub-horizontal plate (depth 140 m, dim 25x500x800 m) with conductive overburden.

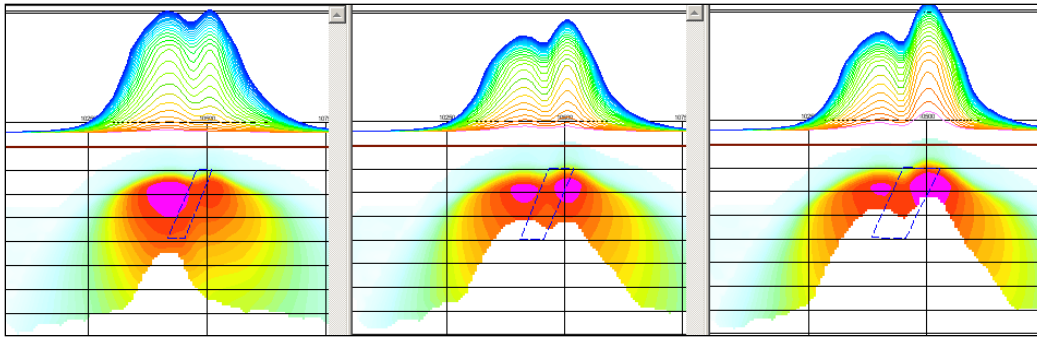


Figure K-9. Maxwell plate models and RDIs from the calculated response for “thick” dipping plates (35, 50, 75 m thickness), depth 50 m, conductivity 2.5 S/m.

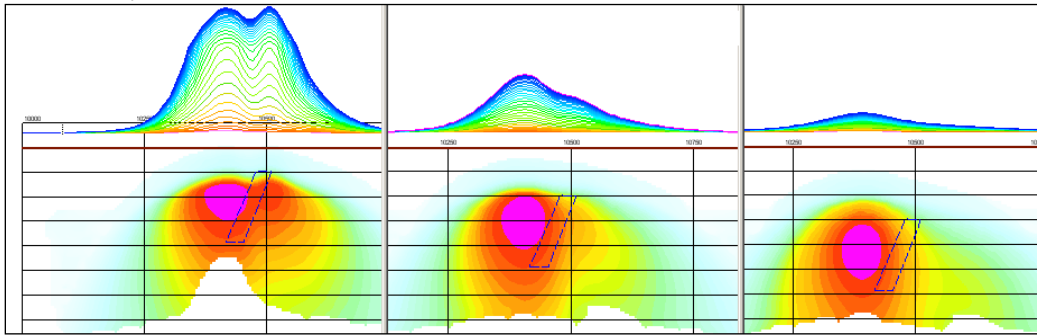


Figure K-10. Maxwell plate models and RDIs from the calculated response for “thick” (35 m thickness) dipping plate on different depth (50, 100, 150 m), conductivity 2.5 S/m.

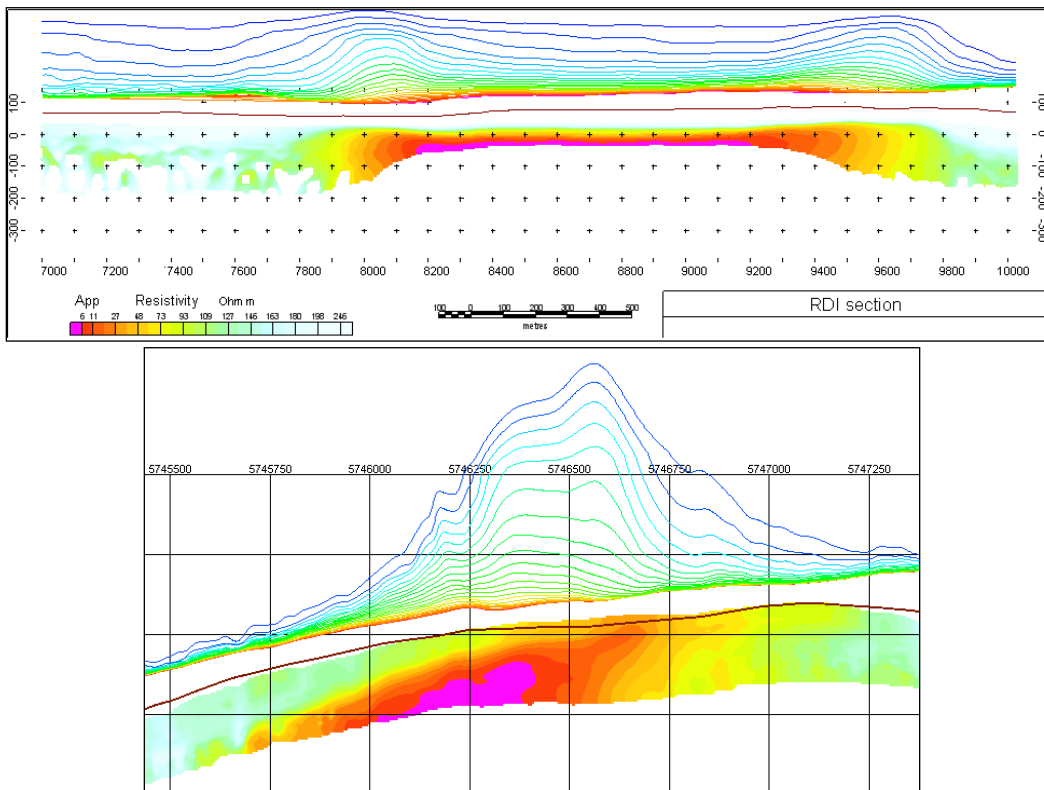
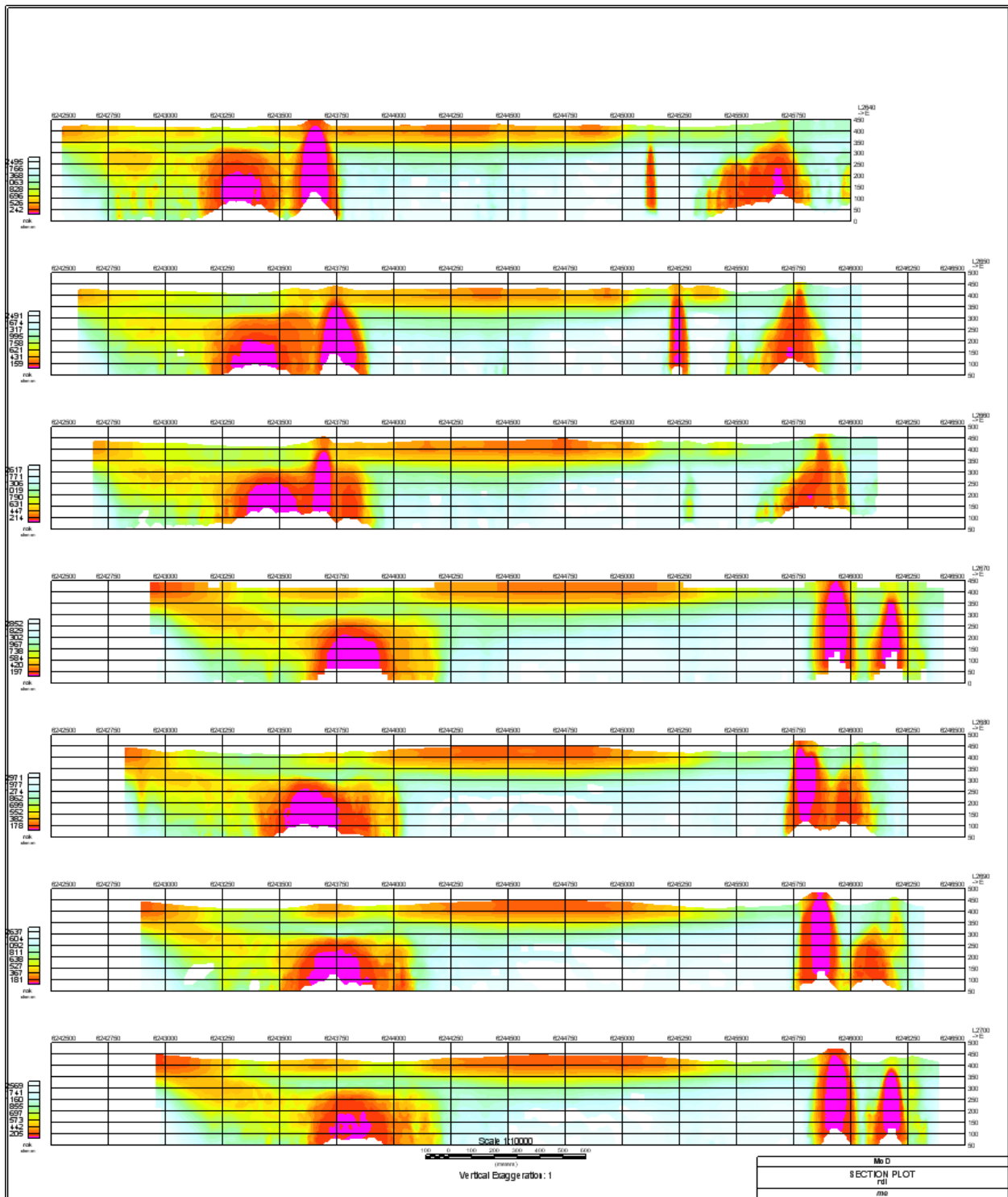


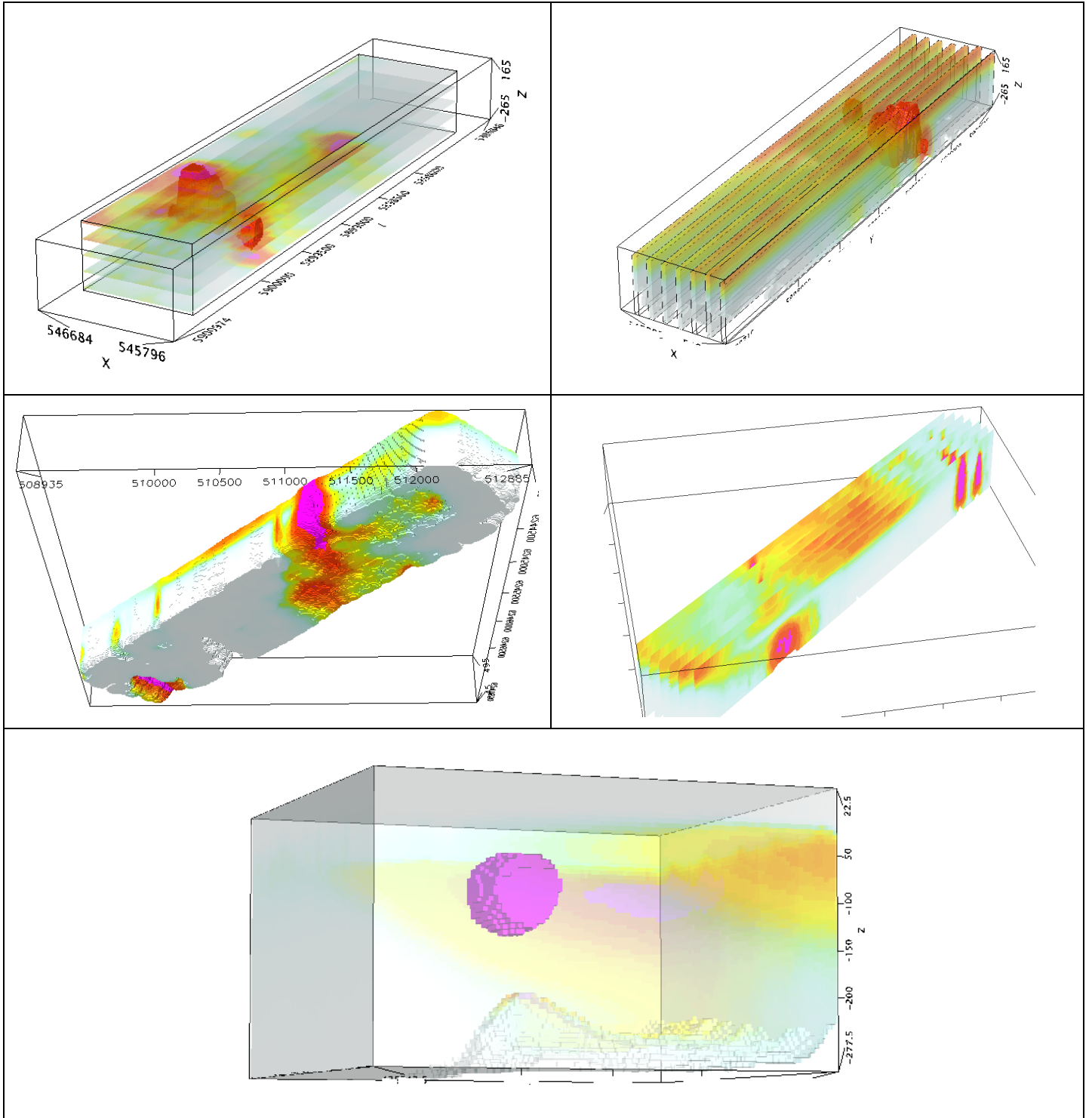
Figure K-11. RDI section for the real horizontal and slightly dipping conductive layers

FORMS OF RDI PRESENTATION

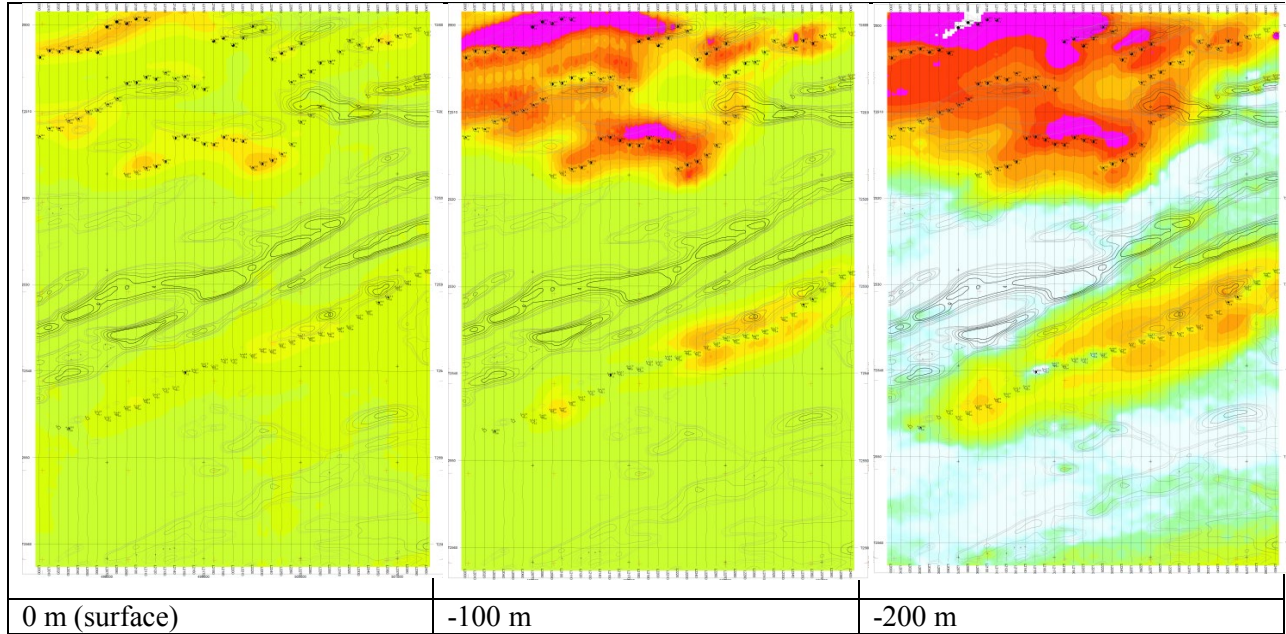
Presentation of series of lines



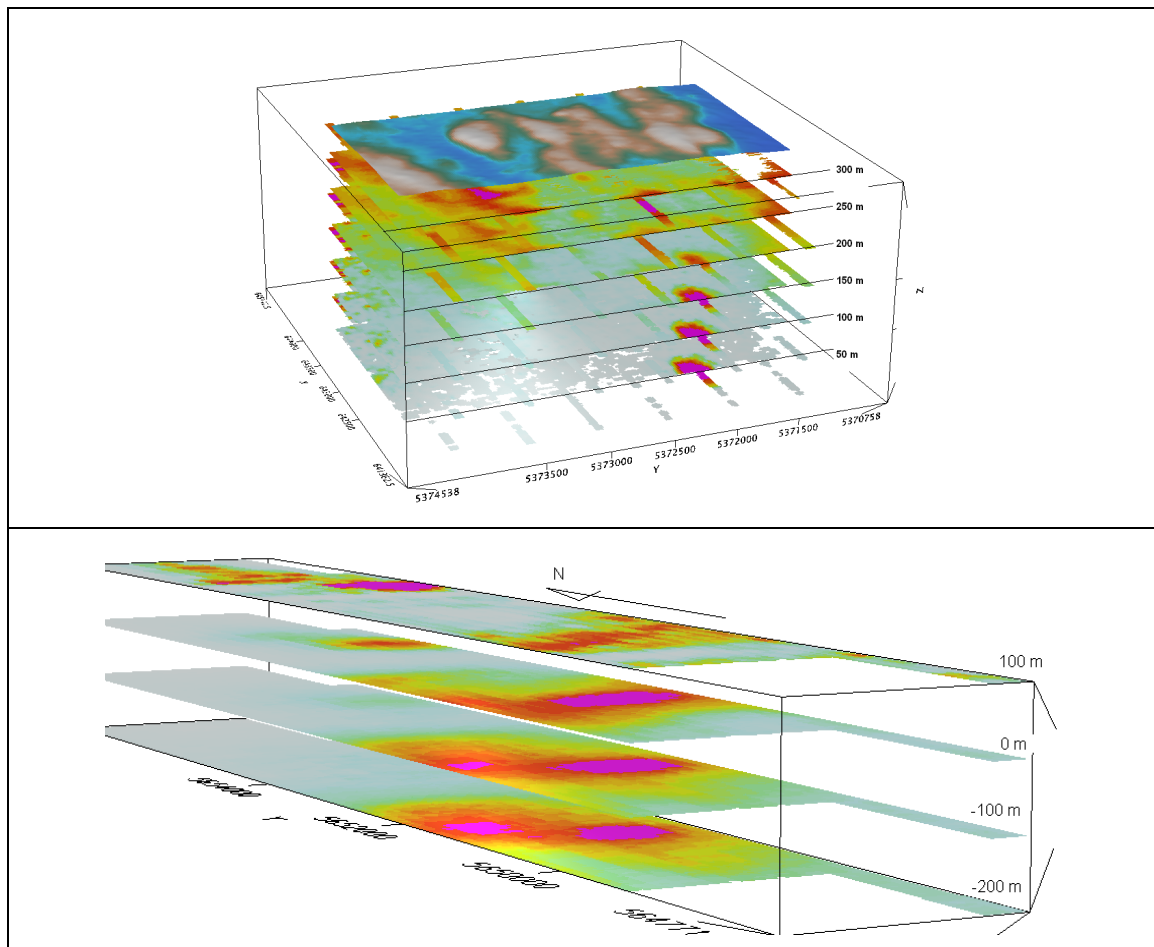
3D presentation of RDIs



Apparent Resistivity Depth Slices plans

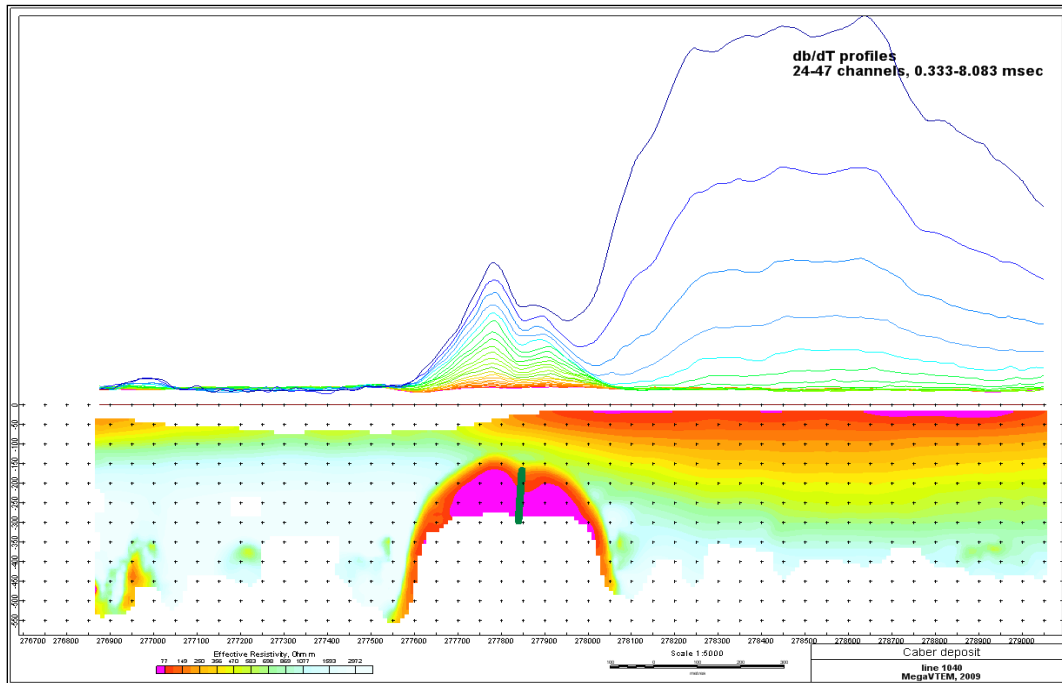


3d views of apparent resistivity depth slices

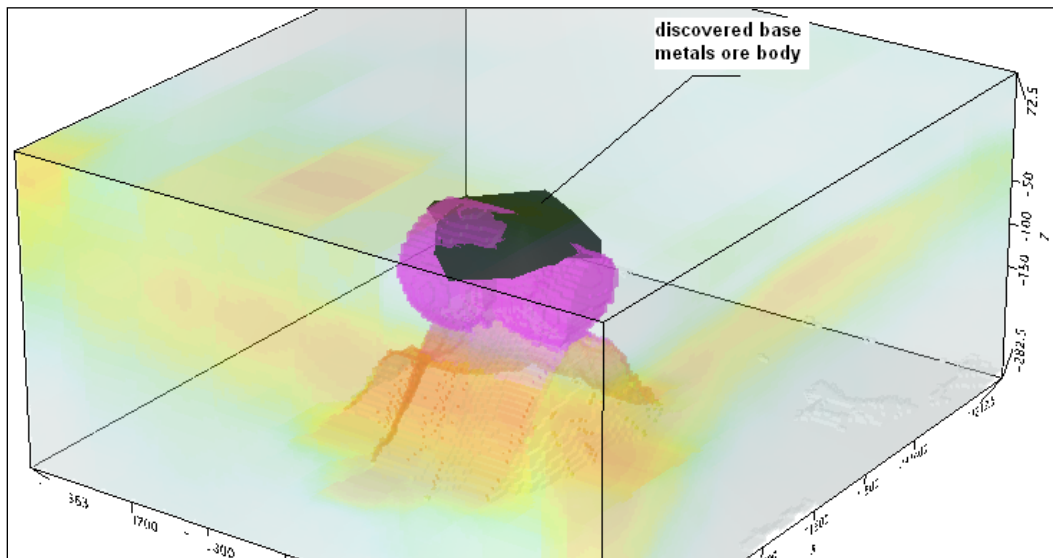


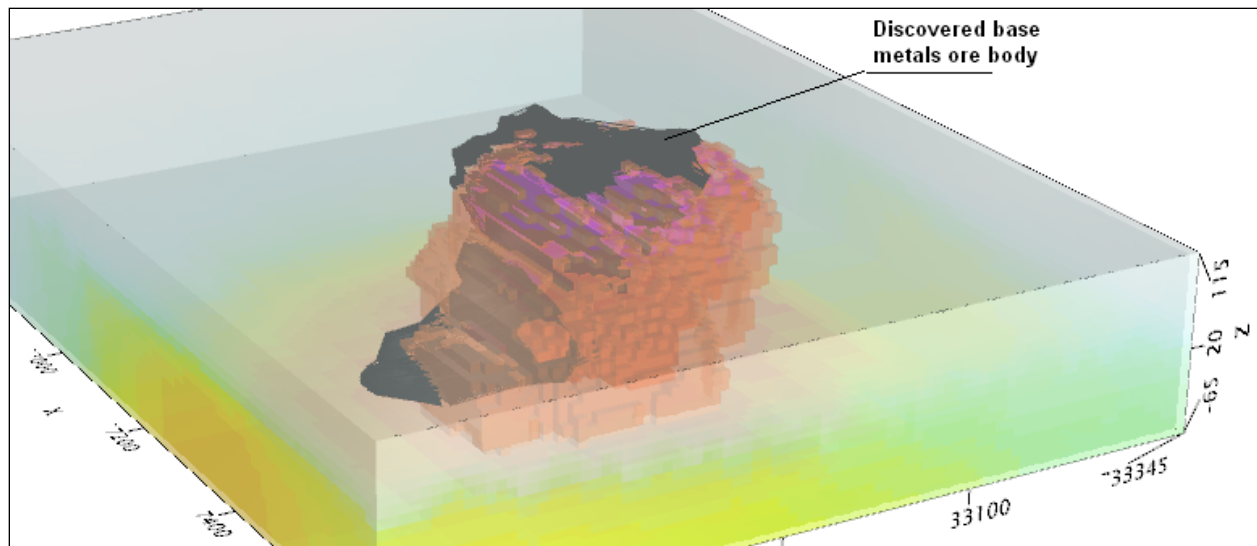
Real base metal targets in comparison with RDIs:

RDI section of the line over Caber deposit (“thin” subvertical plate target and conductive overburden).



3-D RDI voxels with base metals ore bodies (Middle East):





Alexander Prikhodko, PhD, *P. Geo.*
Geotech Ltd.
April 2011

Appendix L. TEST SITES AND CALIBRATIONS

Bourget Test Site

The Bourget test is flown to ensure that the aeromagnetic system measures the total field values with an absolute accuracy of 10 nT or less after the aircraft has been compensated. This test requires that data is recorded coincidentally with the data from the nearby Ottawa magnetic observatory.

With the magnetic sensor at 1000 feet, the 4 cardinal headings are flown, repeating the entire test twice for a total of 8 passes. The test was performed on January 9, 2014 as presented in Figure L-1.



Figure L-1. Bourget Test lines on Google Earth™ (January 9, 2014).

**AEROMAGNETIC SURVEY SYSTEM CALIBRATION TEST RANGES
AT BOURGET, ONTARIO w/TX On**

AIRCRAFT TYPE AND REGISTRATION: C-FK0I DATE: 14/01/2014 DD/MM/YYYY
 ORGANIZATION (COMPANY): Geotech Limited HEIGHT FLOWN: 1000 FEET
 MAGNETOMETER TYPE: G-822A SAMPLING RATE: 10 / SECOND
 MAGNETOMETER SERIAL NUMBER: C2202, s/n75373 DATA ACQUISITION SYSTEM: Geotech DAQ
 COMPILED BY: N. Fiset GSC 12/99

Direction of flight across the Crossroads	Time that Survey Aircraft was over the Crossroads (HH/MM/SS) Greenwich Mean Time	Total Field Value (nT) Recorded in Survey Aircraft over Crossroads (T1)	Observatory Diurnal Reading at Previous 5 Second (T2) from Printout	Observatory Diurnal Reading at Subsequent 5 second (T3) from Printout	Interpolated Observatory Diurnal Reading at Time	Calculated Observatory Value T5 = T4 - C*	Error Value T6 = T1 - T5
EXAMPLE	20:34:40 Z	56840.4 nT	57397.5 nT	57398.3 nT	57398.0 nT	56842.0 nT	-1.6 nT
1001 N	20:00:17.5	54072.1			54618.84	54068.84	3.22
1000 S	19:56:08.6	54073.1			54619.06	54068.96	4.19
2001 E	20:18:27.9	54073.7			54618.99	54068.89	4.84
2000 W	20:14:30.5	54072.4			54618.86	54068.76	3.68
1003 N	20:08:29.3	54075.1			54620.30	54070.30	4.84
1002 S	20:04:19.3	54074.6			54619.35	54069.35	5.24
2003 E	20:26:33.4	54072.6			54617.87	54067.77	4.79
2002 W	20:22:38.1	54071.0			54618.00	54068.00	3.03

*C is the difference in the total field between the Blackburn or Meanook Observatory value (O) and the value (B) at the point above the crossroads at a given height. Blackburn Observatory: 1000 Feet, C = (O-B) = 550 nT; 500 Feet, C = 556 nT
 Meanook Observatory: 1000 Feet, C = (O-B) = 0 nT; 500 Feet, C = 0 nT Total = 33.83 nT

Average North-South Heading Error (T6 North - T6 South) = -0.7 nT
 Average East-West Heading Error (T6 East - T6 West) 1.5 nT Number of Passes for Average = 8 4.23 nT

The completed document must be forwarded to the GSC Project Leader prior to the start of field operations and a copy must be attached to the next weekly report.

**AEROMAGNETIC SURVEY SYSTEM CALIBRATION TEST RANGES
AT BOURGET, ONTARIO w/TX Off**

AIRCRAFT TYPE AND REGISTRATION: C-FK0I DATE: 14/01/2014 DD/MM/YYYY
 ORGANIZATION (COMPANY): Geotech Limited HEIGHT FLOWN: 1000 FEET
 MAGNETOMETER TYPE: G-822A SAMPLING RATE: 10 / SECOND
 MAGNETOMETER SERIAL NUMBER: C2202, s/n75373 DATA ACQUISITION SYSTEM: Geotech DAQ
 COMPILED BY: N. Fiset GSC 12/99

Direction of flight across the Crossroads	Time that Survey Aircraft was over the Crossroads (HH/MM/SS) Greenwich Mean Time	Total Field Value (nT) Recorded in Survey Aircraft over Crossroads (T1)	Observatory Diurnal Reading at Previous 5 Second (T2) from Printout	Observatory Diurnal Reading at Subsequent 5 Second (T3) from Printout	Interpolated Observatory Diurnal Reading at Time H hours + M mins + S sec	Calculated Observatory Value T5 = T4 - C*	Error Value T6 = T1 - T5
EXAMPLE	20:34:40 Z	56840.4 nT	57397.5 nT	57398.3 nT	57398.0 nT	56842.0 nT	-1.6 nT
1001 N	20:39:07.7	54072.2			54618.14	54068.14	4.06
1000 S	20:35:08.9	54071.4			54616.84	54066.84	4.53
2001 E	20:57:32.5	54072.2			54618.00	54068.00	4.21
2000 W	20:53:34.2	54071.7			54617.71	54067.71	4.04
1003 N	20:47:17.5	54072.8			54618.79	54068.79	4.00
1002 S	20:43:04.9	54072.3			54617.97	54067.97	4.36
2003 E	21:06:12.1	54074.0			54619.73	54069.73	4.26
2002 W	21:02:09.4	54073.6			54619.66	54069.66	3.95

*C is the difference in the total field between the Blackburn or Meanook Observatory value (O) and the value (B) at the point above the crossroads at a given height. Blackburn Observatory: 1000 Feet, C = (O-B) = 550 nT; 500 Feet, C = 556 nT
 Meanook Observatory: 1000 Feet, C = (O-B) = 0 nT; 500 Feet, C = 0 nT Total = 33.41 nT

Average North-South Heading Error (T6 North - T6 South) = -0.42 nT
 Average East-West Heading Error (T6 East - T6 West) = 0.24 nT Number of Passes for Average = 8 4.18 nT

The completed document must be forwarded to the GSC Project Leader prior to the start of field operations and a copy must be attached to the next weekly report.

Reid-Mahaffy Test Site

The Reid-Mahaffy test, located near Timmins, is flown as a prerequisite to all surveys for the Government of Ontario Ministry of Northern Development and Mines (MNDM) to ensure that the airborne electromagnetic system is operational and responds to a broad range of electromagnetic responses at different depths below surface.

Sixteen (16) traverse lines are flown at 200 m line spacing oriented in the survey direction. Four (4) tie-lines are flown perpendicular to traverse lines, as indicated in the tables below and figure L-2. The test was performed with EM bird terrain clearance of 30 m. These lines were flown on January 18, 2014.

Line orientation for the Reid–Mahaffy Test.

Traverse lines

Traverse lines	Direction
10	N to S
20	S to N
30	N to S
40	S to N
50	N to S
60	S to N
70	N to S
80	S to N
90	N to S
100	S to N
110	N to S
120	S to N
130	N to S
140	S to N
150	N to S
160	S to N

Tie lines

Tie lines	Direction
9010	W to E
9020	E to W
9030	W to E
9040	E to W

On the location of line 40, 5 additional lines are flown in north-south direction at different level of EM bird terrain clearance: 50 m, 75 m, 100 m, 125 m and 150 m, as indicated in table below. These lines were flown on January 20, 2014.

EM bird terrain clearance on line 40, Reid–Mahaffy Test

Location of L40	EM bird altitude (m)
4050	50
4075	75
4100	100
4125	125
4150	150

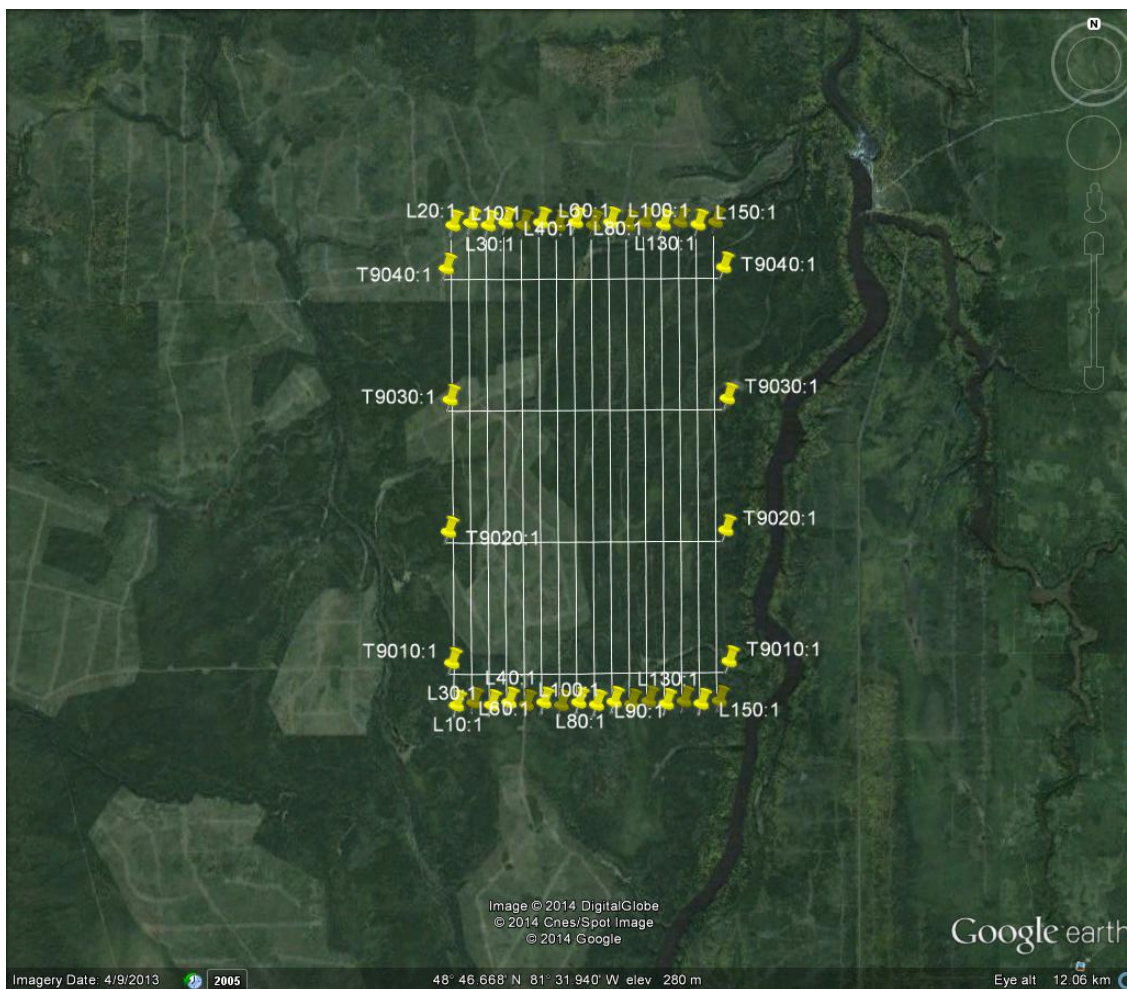


Figure L-2. Reid–Mahaffey Test lines on Google Earth™ (January 18 and 20, 2014).

Data acquired in Reid–Mahaffey was processed and presented in a Geosoft database and grids. Additional products include the selection of anomalies, resistivity-depth images (RDI) and apparent conductivity depth slices.

High Altitude Calibration

The high altitude calibration is conducted on each survey flight. At the beginning and at the end of each flight the helicopter climbs at 1000 feet above ground to check the EM “zero level”.

A graphical representation of a VTEM waveform is shown in Figure 5. A data set in Geosoft GDB format is provided in the final archive containing high altitude test data.

Aluminum Plate Test

This test is performed on ground to verify the sensitivity of the system. An aluminium plate of known conductive response is positioned in alternated positions (vertical and horizontal) for about 10 seconds for 3 time measurements. Response of corresponding dB/dt and Bfield data is then verified.

The Plate test was performed weekly. Result of the test performed on March 2, 2014 is presented in a Geosoft database view below.

When the aluminum plate is horizontal with respect to the loop, measured signal will show positive response, indicating a proper polarity (see H1, H2, H3 in Figure L-3).

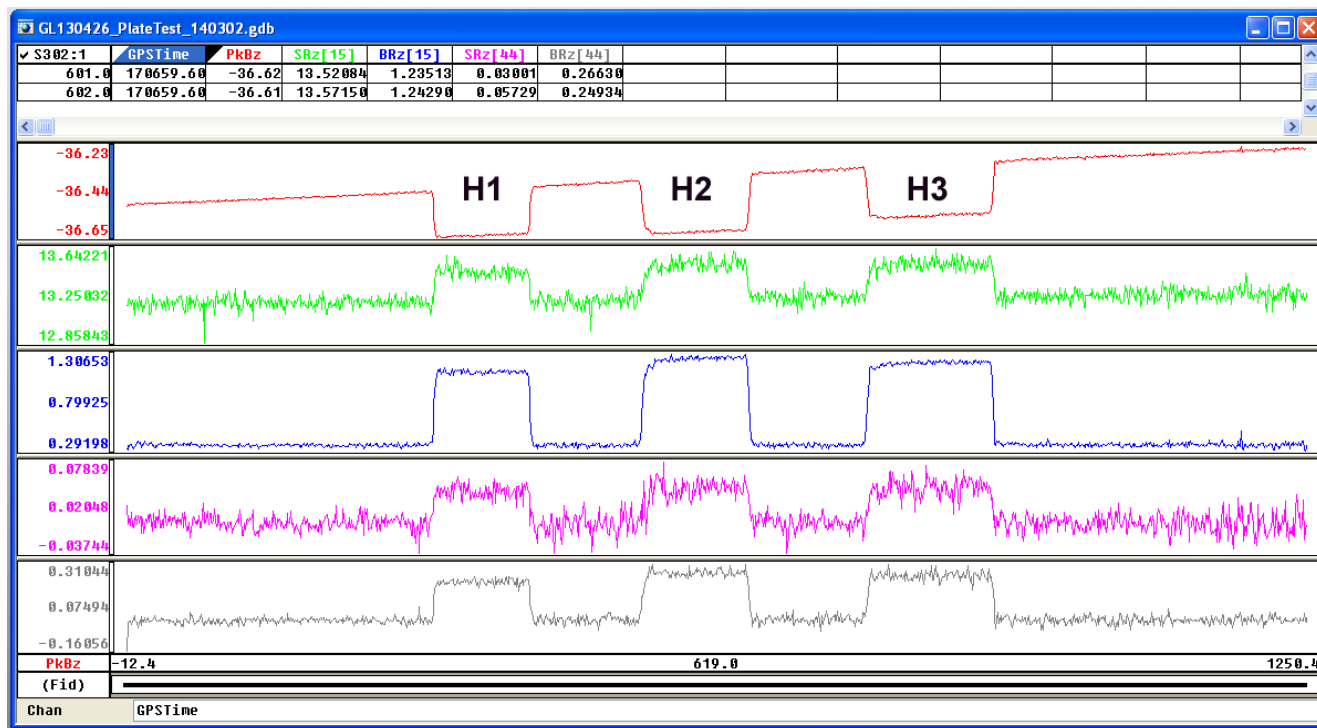


Figure L-3. Plate test results performed on March 2, 2014.

Radar Altimeter Calibration Test

The purpose of the radar altimeter calibration is to verify the performance of radar altimeter readings using the GPS elevation data as the reference.

The calibration is performed flying over the same spot at various altitudes, ranging from 80 m (265 feet) to 150 m (495 feet). The selected spot has known elevation and flat terrain. This test was performed on January 25, 2014 at the beginning of the survey (Figure L-4) and at the end of the survey on March 2, 2014.

As observed in the graphical results presented below, where the GPS elevations versus radar readings are plotted, the relationship between radar and GPS readings are linear, and the radar readings are very accurate ($R^2 \sim 1.0$), for the range of flying heights to be expected for the survey.

Radar checks were performed once per day. These checks consisted of the ground crew communicating with the operator/pilot via radio when the tail of the system would leave the ground.

Radar Altimeter Calibration Test

Project:	GL130426
Location:	Nestor Falls, Ont.
Date:	25-Jan-14
Flight:	1
Test No.	1
Aircraft:	C-FKOI

Line	Nominal Altitude above ground (m)	Nominal Altitude above ground (ft)	Radar Altitude Raw Data (m)	DGPS Altitude Ellipsoidal Height (m)	DTM = DGPS - Radar Alt Ellipsoidal Height WGS84 (m)	DGPS Altitude (ALT) ALT=DGPS - AVERAGE(DTM) (m)
1080	80.00	262.5	80.9	426	345.10	79.96
1085	85.00	278.9	86.02	431.3	345.28	85.26
1090	90.00	295.3	89.73	435.1	345.37	89.06
1100	100.00	328.1	100.2	446.3	346.10	100.26
1120	120.00	393.7	121.14	467.9	346.76	121.86
1150	150.00	492.1	152.25	499.9	347.65	153.86
					346.04	
					AVERAGE	

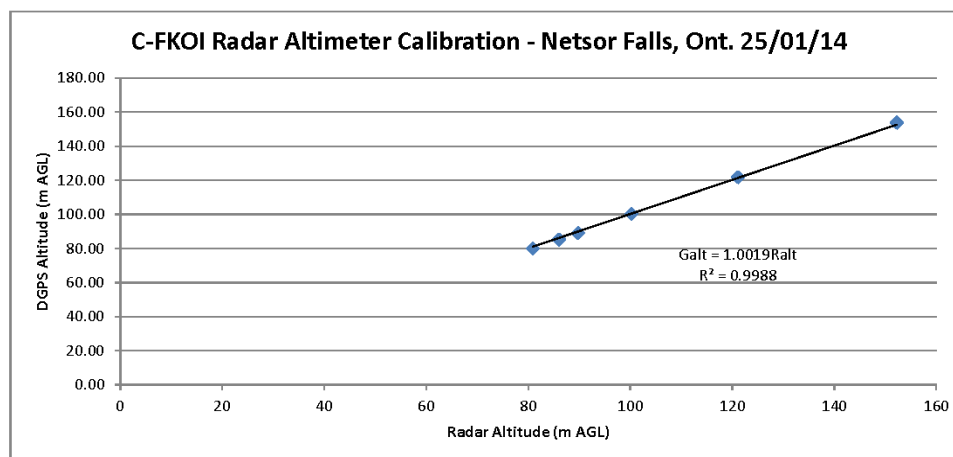


Figure L-4. Radar altimeter test results performed on January 25, 2014.

Magnetometer Cloverleaf Tests

Calibration flights are performed to verify the heading errors of the magnetometer in the 4 cardinal directions. The TDEM data is analyzed during this process as well to confirm data quality in terms of response to turns and varying wind conditions.

This test is performed once per month. Two tests were performed during this survey: February 8 and March 2, 2014 (Figures L-5 and 6).

Test Date: February 8, 2014

Test Location: Nestor Falls

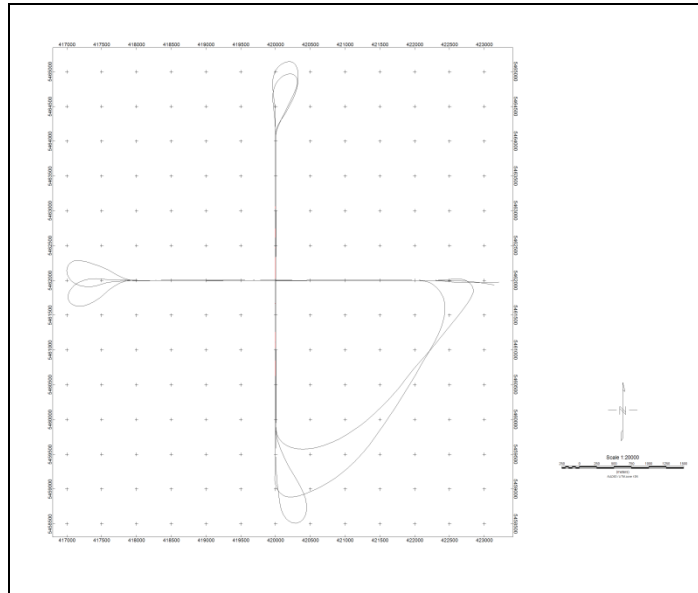
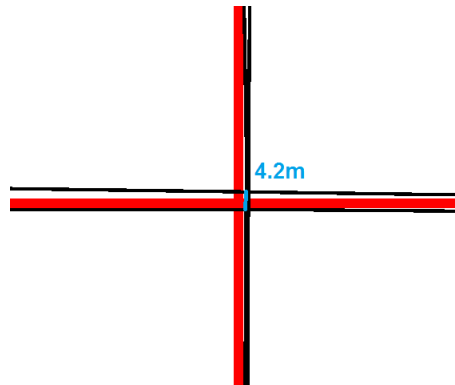


Figure L-5. Flight path of Heading test performed on February 8, 2014.

INTERSECTION 1: EM TRANSMITTER ON
 Black lines indicate flight path flown, red lines indicate ideal flight path.



RAW DATA

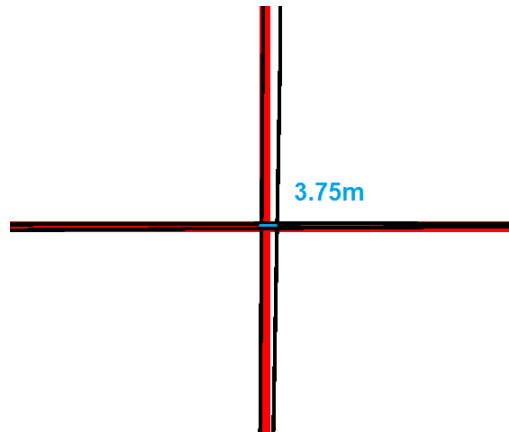
(MAG2 is diurnal corrected value of Total Magnetic Intensity)

Direction	Line #	Fiducial	Mag2
90	S090_1	16325.0	56947.72
180	S180_1	22546.0	56948.08
270	S270_1	13916.0	56947.78
360	S360_1	19900.0	56947.81

HEADING EFFECT COEFFICIENTS

Direction	Heading Correction
90	0.13
180	-0.23
270	0.07
360	0.04

INTERSECTION 2: EM TRANSMITTER OFF
 Black lines indicate flight path flown, red lines indicate ideal flight path.



RAW DATA

(note: MAG2 is diurnal corrected value of Total Magnetic Intensity)

Direction	Line #	Fiducial	Mag2
90	S090_2	33877.0	56947.80
180	S180_2	27946.0	56947.88
270	S270_2	31477.0	56947.88
360	S360_2	25465.0	56947.62

HEADING EFFECT COEFFICIENTS

Direction	Heading Correction
90	-0.01
180	-0.08
270	-0.08
360	0.17

1) Test Date: March 2, 2014

Test Location: Nestor Falls

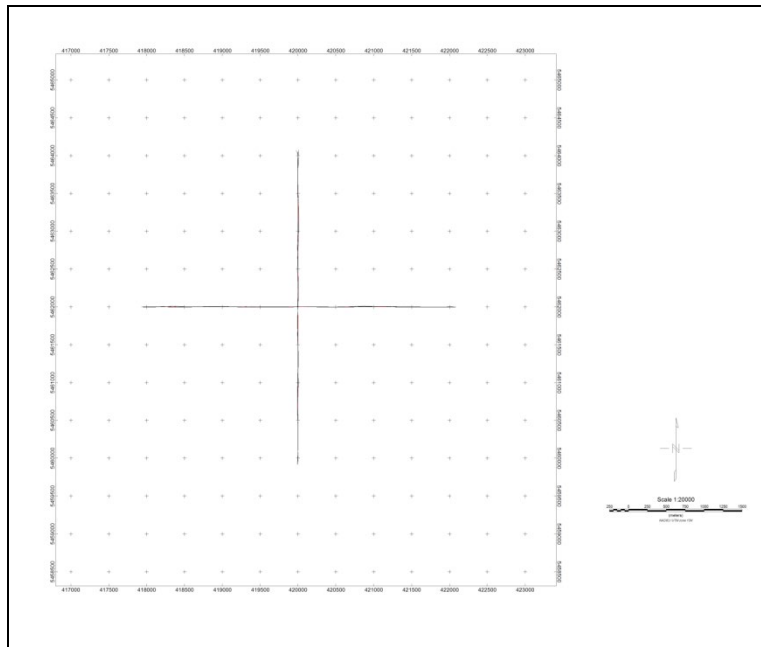
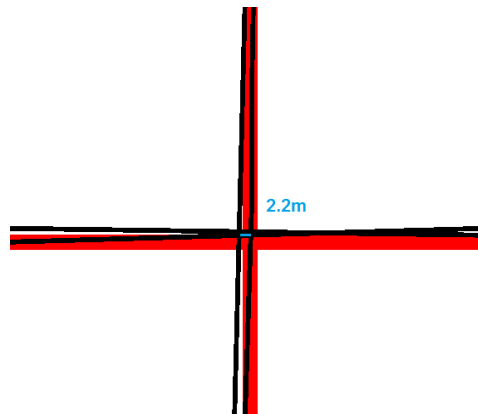


Figure L-6. Flight path of Heading test performed on March 2, 2014.

INTERSECTION 1: EM TRANSMITTER ON
 Black lines indicate flight path flown, red lines indicate ideal flight path.



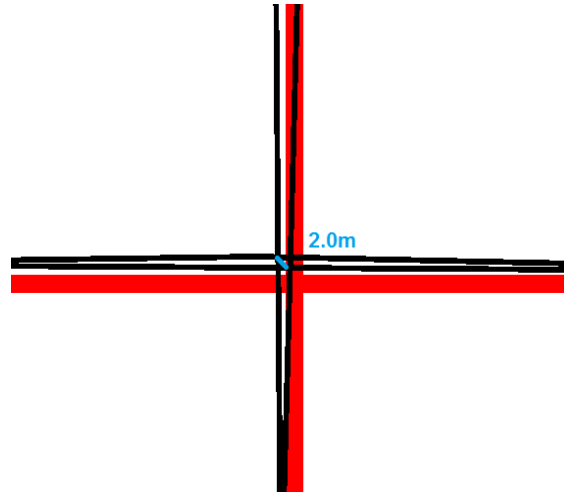
RAW DATA
 (MAG2 is diurnal corrected value of Total Magnetic Intensity)

Direction	Line #	Fiducial	Mag2
90	90_TxOn	72879.0	56947.66
180	180_TxOn	78150.0	56947.85
270	270_TxOn	67784.0	56948.05
360	360_TxOn	82372.0	56948.17

HEADING EFFECT COEFFICIENTS

Direction	Heading Correction
90	0.27
180	0.08
270	-0.12
360	-0.24

INTERSECTION 2: EM TRANSMITTER OFF
 Black lines indicate flight path flown, red lines indicate ideal flight path.



RAW DATA

(note: MAG2 is diurnal corrected value of Total Magnetic Intensity)

Direction	Line #	Fiducial	Mag2
90	90_TxOff	92598.0	56947.60
180	180_TxOff	85522.0	56948.04
270	270_TxOff	95103.0	56948.12
360	360_TxOff	88407.0	56947.74

HEADING EFFECT COEFFICIENTS

Direction	Heading Correction
90	0.28
180	-0.17
270	-0.25
360	0.14